2014

P115-SNARE INTERACTIONS REVEAL A NEW MODEL OF FUNCTION FOR THE TETHERING FACTOR P115

Ting Wang
The University of Montana

P115-SNARE INTERACTIONS REVEAL A NEW MODEL OF FUNCTION FOR THE TETHERING FACTOR P115

BY

TING WANG

NOVEMBER 2014

B.S., CHINA PHARMACEUTICAL UNIVERSITY, NANGJING, CHINA, 2007

A DISSERTATION

SUBMITTED TO THE DEPARTMENT OF BIOLOGICAL SCIENCES

PRESENTED IN PARTIAL FULFILLMENT OF THE REQUIREMENTS

FOR THE DEGREE OF

DOCTOR OF PHILOSOPHY

INTEGRATIVE MICROBIOLOGY AND BIOCHEMISTRY, CELLULAR AND MOLECULAR BIOLOGY

THE UNIVERSITY OF MONTANA

MISSOULA, MT

Approved by:

Jesse Hay, Chair

Division of Biological Sciences

Mark Grimes

Division of Biological Sciences

Michele McGuirl

Division of Biological Sciences

Stephen Sprang

Division of Biological Sciences

Erica Woodahl

Department of Biomedical & Pharmaceutical Sciences

Abstract

Wang, Ting, Ph.D., Fall 2014 Cell and molecular Biology

P115-SNARE interactions reveal a new model of function for the tethering factor p115.

Chairperson: Jesse Hay

The endomembrane system consists of several connected yet distinct compartments, constantly exchanging material via the flow of membrane-enclosed vesicles. Protein transport between the endoplasmic reticulum (ER) and the Golgi is one of the most fundamental trafficking pathways in eukaryotic cells, as well as the first step in the secretory pathway. The fusion between vesicles and target membranes requires the orchestration of tethers, Rabs, SM proteins and SNAREs. Tethering factors regulate the targeting of membrane-enclosed vesicles and enhance the efficiency as well as specificity of membrane fusion. P115, a Golgin family tether, has been shown to participate in multiple stages of ER/Golgi transport. Despite extensive study, p115's mechanism of action is poorly understood. SNARE proteins make up the machinery for membrane fusion, and strong evidence shows that p115's function is directly linked to its interaction with SNAREs. Using a gel filtration binding assay, we have demonstrated that in solution p115 stably interacts with ER/Golgi SNAREs rbet1 and sec22b, but not membrin and syntaxin 5. These binding preferences stemmed from selectivity of p115 for monomeric SNARE motifs as opposed to SNARE oligomers. Soluble monomeric rbet1 can compete off p115 from COPII vesicles. Furthermore, excess p115 inhibits p115 function in trafficking. We conclude that monomeric SNAREs are a major

binding site for p115 on COPII vesicles, and that p115 dissociates from its SNARE partners upon SNARE assembly. Our results suggest a model in which p115 forms a mixed p115/SNARE helix bundle with a monomeric SNARE, facilitates the binding activity and/or concentration of the SNARE at pre-fusion sites, and is subsequently ejected as SNARE complex formation and fusion proceed.

Acknowledgements

First and foremost I would like to thank my advisor Jesse Hay, who is the best mentor a student could hope for. Always patient and encouraging, he has taught me the principles of being a good scientist, and has provided constant support throughout my research.

I thank my Committee members Mark Grimes, Stephen Sprang, Michele McGuirl, Erica Woodahl, and Katie George. They have given inspiring advice for my project, and have always managed to find time for committee meetings despite busy schedules.

I would like to thank the Hay lab members Marvin Bentley, Nandhakumar Thayanidhi, Meg Trahey, Jared Helm, and Deborah Nycz, for their support, friendship, and insightful questions during my time in the lab. I also thank Robert Grabski in the Sztul lab at UAB, for contributing one critical piece of data to this study; and Dr. Elizabeth Sztul, for reviewing and editing my paper.

A special thanks to Dr. Stephen Lodmell and Dr. Walter Hill, who taught me everything I know about nucleic acids; and to Dr. Scott Wetzel, who took the pain of reviewing my (slow) progress every year.

Last but not least, I would like to give my thanks to Sherrie Wright, Jill Burke, Janean Clark, Teri Daniels, Robin Hamilton, and other personnel of the DBS office, who always provided help when needed.

The work presented in this thesis was funded by NIH. Sections of this thesis were adapted from Wang, T et al. (2014). "p115-SNARE Interactions: A Dynamic

Cycle of p115 Binding Monomeric SNARE Motifs and Releasing Assembled Bundles." Traffic.

Table of Contents

List of Figures

List of Tables

Chapter I: Introduction

A. The Secretory Pathway Overview

The eukaryotic secretory pathway provides the foundation for many cellular processes. The endomembrane system consists of several connected yet distinct compartments, constantly exchanging material via the flow of membrane-enclosed vesicles. Proteins and other essential molecules are transported to their destinations throughout the cell by these vesicles. Vesicles containing sorted cargo are generated by one compartment, attached to microtubules, and moved to another compartment. Upon arrival, vesicle membranes fuse with the membranes of the target compartment, and the content of vesicles are released into the organelle lumen. The sorting of cargo, budding of vesicles, and the eventual membrane fusion comprise a sequence of tightly regulated and highly specific individual steps that are carried out through the orchestration of different families of proteins [1].

The endoplasmic reticulum is considered the 'gate' to the secretory pathway. ER is the entry point for newly synthesized proteins, directed by an ER signal sequence [2]. After being sorted in the ER, proteins are moved in COPII coated vesicles to the Golgi apparatus, where they receive further modification and are either retained, cycled back to the ER, or transported to other parts of the cell. The Golgi therefore provides an important connecting point for other branches of the secretory pathway, including the exo- and endocytosis [Figure 1].

Anterograde transport from ER to Golgi consists of the flow of COPII-coated vesicles [1, 3]. Sculpted from ER membrane, these spherical vesicles undergo homotypic fusion and give rise to an intermediate compartment between the ER and

Golgi, termed versicular tubular cluster (VTC). VTCs then move along microtubules towards the Golgi, during which process anterograde cargoes are further concentrated as ER-localized proteins, export machinery, and excess membrane are returned to the ER.

B. Key Components of the Secretory Pathway

a. Coat proteins

Coat proteins are important components involved in cargo recruitment and membrane remodeling during the budding of vesicles. Coatomers assemble into cage-like structures on a specific membrane patch, bending the membrane and eventually 'sculpt out' spherical vesicles from the donor membrane. There are three major groups of coatomers: COPI, COPII, and Clathrin [4]. In general, coatomer cages are assembled by proteins containing the α-solenoid domain and the β-propeller domain, even though the detailed architecture of the cages are distinct [5]. The COPI coat consists of 7 subunits (α, β, β′, ε, γ, δ, and ζ), and the coated vesicles carry out retrograde ER-Golgi transport as well as intra-Golgi transport [6]. The COPII coat is assembled by Sec13, Sec31, Sec23, and Sec24 at the ER exit site, and COPII-coated vesicles mediate anterograde ER-Golgi transport [7, 8]. The Clathrin coat, assembled by clathrin heavy chains (CHCs) and clathrin light chains (CLCs), has been implicated to play a part in multiple trafficking pathways, including endocytosis and protein sorting in the trans-Golgi network [9, 10, 11]. The assembly of coats is typically regulated by membrane-anchored GTP-binding proteins (e. g. Sar1 for COPII, Arf1 and -3 for COPI and Clathrin) [11].

b. SNARE proteins

A group of proteins termed soluble N-ethylmaleimide-sensitive fusion protein (NSF) attachment protein receptors (SNAREs) play an especially important role in vesicle trafficking. SNAREs are responsible for catalyzing the merger of membranes. The assembly of SNARE complexes overcomes the energy barrier and directly brings the opposing membranes together, which leads to fusion. SNAREs are characterized by a homologous domain called the SNARE motif, which spans approximately 60~70 residues [12]. The monomeric SNARE motif is usually unstructured, yet it adopts an α-helical conformation when it enters into a SNARE complex [12, 13]. For most SNARE proteins, the SNARE motif is sandwiched between an N-terminal domain and a C-terminal transmembrane domain (or other type of membrane-anchor, such as palmitoylation or prenylation) [12].

The formation of the SNARE complex involves the SNARE motifs of four cognate SNARE proteins. The assembly of SNARE complexes starts from the N-termini of the SNARE motifs, and proceeds through the lengths of the domains in a 'zipping up' motion [14]. Through the SNAREs' C-terminal membrane anchors, the assembly of the four-helix bundle pulls the opposing membranes close together, dehydrating the apposed membrane bilayers, initiating lipid mixing between membranes as well as the formation of a fusion pore, the expansion of which ultimately results in bilayer fusion [14, 15, 16]. The eventual product of SNARE assembly is an ultra-stable complex consisting of four parallel-aligned α-helices, sustained by multiple-layer hydrophobic interactions [17]. A single polar layer,

termed the 0 layer, exists in the central region of the four-helix bundle. One of the SNARE motifs contributes an arginine (R) residue to the layer, which engages in hydrogen bonds with three glutamine (Q) residues contributed by the other three SNARE motifs. SNARE proteins can thus be classified into R- and Q- SNAREs. Based on their positions in the SNARE complex, Q-SNAREs can be further grouped into Qa, Qb, and Qc subtypes [18].

Utilizing energy from ATP hydrolysis, the SNARE complex can be disassembled by the chaperone NSF and its co-factor α-SNAP [19, 20]. The recycled SNAREs can participate in further membrane fusion events [Figure 2].

Sec1/Munc18-like (SM) proteins are a group of proteins that facilitate SNAREs in fusion. The typical structure of SM protein resembles a U-shaped 'clasp' [21, 22], and appears to function as a clasp for the four-helix bundle SNARE complex [22]. SM proteins bind the 'closed' four-helix conformation of syntaxins as well [21], but they also contain an additional binding site for a N-terminal peptide of the syntaxin H_{abc} domain [21, 23]. This interaction possibly anchors the SM protein to the SNARE complex, leaving the 'U' part of SM protein free to interact transiently with and stabilize the forming four-helix bundle [22].

These interactions suggest a regulatory role for SM proteins in SNARE complex assembly or/and disassembly [22]. Due to their multiple binding sites on SNAREs, the exact functions of SM proteins are not clear. There is also evidence suggesting that SM proteins can 'proofread' SNAREs [24, 25], by disassembling the wrongly-paired SNAREs and stabilizing cognate SNARE complexes [24].

Another important feature of SNARE proteins is the N-terminal domain. Unlike the homologous SNARE motif, despite some sequence or/and structural homology shared between certain groups of SNAREs (i. e. the syntaxin family [26, 27]), the structure and function of the N-terminal domain varies among SNAREs. Three-helix bundle is a very common conformation, and the ER-Golgi SNARE membrin has this type of N-terminal domain. The N-terminal domains of syntaxins also adopt an antiparallel three-helix bundle conformation [28], and are termed H_{abc} domains. These domains possess affinities for their respective SNARE motifs, and the intramolecular interactions appear to regulate the activity of the syntaxin SNARE motif. The removal of syntaxin 5 N-terminal domain greatly enhances the incorporation of syntaxin 5 into SNARE complexes [29]. Similar effects have been observed for other syntaxins [30, 31], suggesting the N-terminal domain as a potential negative regulator for syntaxin SNARE activities.

Profilin-like folds are found among the N-terminal domains of exocytotic SNARE VAMP7, mammalian neuronal SNARE ykt6, and ER-Golgi SNARE sec22b [32, 33, 34]. Termed longin domains, their functions are not very well understood. It has been reported that the longin domains of VAMP7 and ykt6 negatively regulate their SNARE activities, in the same manner as a syntaxin's N-terminal domain [35]. There is also evidence suggesting that the two longin domains are important for the localization of their respective SNAREs [34-38]. Such specific regulatory or targeting effects, however, have not been observed with sec22b, although the longin domain of sec22b seems to affect the SNARE's ER export [36-38]. The longin domain has also been established as a potential coat-recruitment site [39].

c. Vesicle tethering and tethers

Other key components of the secretory pathway include tether proteins. It has been known since 1998 that SNAREs are required and sufficient for catalyzing the fusion of liposomes [40]. However, the rate of SNARE-only fusion is drastically lower than that of fusion that occurs under physiological conditions. This suggests potential cofactors participating in fusion or its upstream events.

The targeting and tethering of vesicles prior to their fusion greatly enhance fusion's efficiency [41, 42]. Furthermore, although only cognate SNAREs assemble complex efficiently, and in vitro SNARE-mediated liposome fusion has been shown to be highly specific [43, 44], evidence suggests that fusion can be carried out by non-cognate SNAREs as well [45]. Thus, tethering of vesicles confers another degree of specificity to SNARE-mediated fusion. A number of protein factors required for tethering have been identified and characterized, and can be roughly classified into two groups: Proteins that act as an individual rod-like tethers, and proteins that function as a stable part of a multi-component tethering complex.

It was believed that vesicles shed their coats soon after budding, which suggests that coatomers are unlikely to be involved in vesicle tethering and fusion [46]. However, more recent studies have shown that sections of the coat can stay on the vesicles until tethering [47], and coat proteins serve as a potential binding site for tether recruitment. Sec23, a COPII subunit, binds directly to Bet3, one of the core subunits shared between all three transport protein particle (TRAPP) complexes [47, 48], whereas COPI subunit γ-COP interacts with two of TRAPPII-specific

subunits [49]. COPI subunits also interact with the conserved oligomeric Golgi (COG) complex [49], as well as Dsl1 [49].

In addition to coatomers, Rabs and SNAREs also play a part in tether recruitment and localization. Most tethers are Rab effectors (more in the Rab GTPases section). Rab1 recruits tether p115/Uso1p to the COPII vesicles [50], whereas Sec4p directs subunits of the tethering complex exocyst to post-Golgi vesicles [51]. P115's population on COPII vesicles is also affected by SNARE status [52].

First identified as autoantigens, the rod-like tethers include the well-characterized endosomal tether EEA1, as well as the Golgin protein family. The members of this group often form homodimers and are characterized by structurally predominant elongated α-helical coiled-coil domains [53]. Golgins and other rod-like tethers are usually conserved across species, with central helical region and non-helical termini [53, 54]. P115/Uso1p, GM130, and Giantin are some other examples of this group.

Golgins are primarily localized to the Golgi, and their role in maintaining the homeostatsis of Golgi has been extensively studied [55-60]. The exact molecular detail of function for these rod-like tethers, however, is not very well understood. Due to their elongated shape, a ‘vesicles on the strings’ model was proposed [55, Figure 3]. In this model, Golgins assemble into a fibrous matrix (‘strings’) protruding from the surface of Golgi cisternae, the distal ends of which attach to vesicles such that vesicles may be passed between different ‘strings’. This would allow vesicles to be transported between the succesive Golgi stacks without diffusing away.

Extensive coordination between Golgins has been reported, suggesting transport mediated by these proteins is a concerted effort [59, 60].

Several rod-like tethers, in particular p115/Uso1p, are not restricted to the Golgi and have a more general role in the secretory pathway. Similar to their hypothetical model of action at the Golgi, in other steps of the secretory pathway, coiled-coil tethers are proposed to form elongated structures and to capture vesicles prior to the docking of SNAREs, and possibly to facilitate the downstream events by catalyzing the assembly of SNARE complexes [49, 62]. Despite their structural similarities, tethers localize to their respective compartments and are specific for each step in the secretory pathway, thus enhancing the overall specificity of vesicle targeting and the membrane fusion system [63] [Figure 4 and Table 1].

On the other hand, a considerable number of tethering factors form multisubunit tethering complexes (MTCs). Usually conserved in yeast and mammals, these complexes contain 3-10 subunits. In most cases, subunits within a tethering complex share a certain level of sequence or structural similarity [64]. Similar to rod-like tethers, tethering complexes are found to participate at every branch of the secretory pathway [64, 65]. Based on sequence homology, the COG, Dsl1, exocyst, and GARP (Golgi-associated retrograde protein) complexes have been collectively given the name complex associated with tethering containing helical rods (CATCHR) family. Structural analysis indicates that many subunits of these MTCs are evolutionarily related [64]. The Non-CATCHR group of MTCs includes the TRAPPs, HOPS (homotypic fusion and protein sorting) complex, and CORVET (class C core vacuole/endosome tethering) complex. Some major and well-studied ER-Golgi

complexes include: TRAPPI, II and III, which are proposed to function in concert with p115/Uso1p, at the late stage of ER-Golgi transport; the COG complex, which primarily functions within the Golgi apparatus [66]; exocyst, which primarily localizes to the trans-Golgi network and participates in the trafficking of post-Golgi vesicles to the plasma membrane [67, 68]; and the COPI vesicle tether Dsl1, whose structure and function has been relatively well characterized [69, 70].

d. Rab GTPases

Rab GTPases also play an important part in membrane transport. As molecular 'switches', Rabs regulate many trafficking processes including cargo recruitment, coat assembly and disassembly, vesicle movement, as well as membrane fusion [71]. In addition, Rabs provide enhanced membrane identity, as exemplified by their role in the specific recruitment of tethering factors [72, 73].

All the aforementioned tethers or tethering complexes, with the exception of Dsl1 and TRAPPs (which are Rab GEFs), are/contain Rab effectors [74]. P115 and GM130 are effectors of Rab1/Ypt1, which has been shown to play a key role in ER-Golgi transport. Giantin, on the other hand, interacts with both Rab1 and Rab6, suggesting an additional regulatory role for this Golgin [75]. The COG tethering complex is the effector of several Golgi Rabs, possibly because COG acts as a central point for multiple retrograde tethering events at Golgi [76]. In addition, Sec4 recruits the exocyst [51], Ypt6/Rab6 binds GARP [77, 78], and HOPS interacts with Ypt7/Rab7, whereas the related CORVET binds the Rab Vps21 [79-81]. Rabs appear to regulate the tethering process by coordinating between various families of

players, such as SM proteins, tethers, and SNAREs [71]. The lack of an identified Dsl1 Rab possibly hints at a different regulatory mechanism for Dsl1 [74].

Recently, the exact role of TRAPP complexes in membrane tethering has been called to question. TRAPPs do not share structural or sequence homology with the CATCHR family, nor the HOPS and CORVET complexes [64]. All MTCs with the exception of Dsl1 are Rab effectors, whereas TRAPPs are Rab GEFs [82]. Evidence suggests that TRAPPs are required for the tethering process [83], yet it is unknown whether TRAPP is capable of binding receptors on both vesicle and target membranes simultaneously [82]. Therefore, it is unclear whether TRAPPs act by directly tethering apposed membranes, or by regulating other tethers' functions through interactions with Rab1.

C. SNARE-Tether Interactions

As upstream regulators and fusion cofactors, almost all known tethers or MTCs can interact with at least one SNARE [62]. P115, as a more 'general' tethering factor, interacts with various ER-Golgi SNAREs (see P115-SNARE interactions below). Other coiled-coil tethers and MTCs also have SNARE binding properties.

It has been shown that interactions between tethers and SNAREs can regulate SNARE activities. GM130's binding to sytnaxin 5 seems to inhibit its incorporation into binary SNARE complex [84]. Sec6, a subunit of the exocyst, interacts with the yeast plasma membrane sec9 [85], and regulates sso1-sec9 binary complex assembly [86]. Cog4, a COG subunit, also interacts with syntaxin 5 and facilitates its SNARE assembly [87]. The endosomal tether EEA1 interacts with trans-Golgi SNARE

syntaxin 6 and endosomal syntaxin 13 [88, 89], and these interactions seem to be required for endosome fusion [90].

Tethers can also regulate the localization of SNARE proteins. Interactions between COG component Cog6 and syntaxin 6 seem to affect syntaxin 6's localization to trans-Golgi [91]. In fact, the COG complex seems to be important for the localization of many Golgi SNAREs [92].

The physiological implications of many tether-SNARE interactions are not entirely clear. However, due to the fact that many tethers or MTCs interact with multiple SNAREs, it is possible that they facilitate SNARE complex assembly by bringing SNAREs together [62]. As for the SNARE motif-binding tethers, it is possible that they function in concert with SM proteins and proofread/stabilize SNARE complexes [94].

D. Research Rationale

a. Tether protein p115

One of the better-studied Golgins, p115, was first identified as a high molecular weight factor required for the docking/tethering step in intra-Golgi vesicular transport and transcytosis [56, 94, 95]. Its yeast homolog, Uso1p, was also required for ER-Golgi transport [94]. These early studies placed p115/Uso1p's action prior to SNARE-mediated membrane fusion [96-99], although later evidence also suggests a downstream role for p115/Uso1p [50, 100].

P115, as a Golgin, exists as a homodimer in the cell [56, 101, 102]. It is localized primarily to the *cis*-face of the Golgi, but has an abundant cytosolic pool as

well [103]. The bovine p115 monomer consists of a globular head domain, which spans residues 1-651, an elongated coiled-coil domain (residues 652-909), and an acidic tail domain (residues 910-961) [101]. Based on primary sequence comparison, the head domain of p115 contains two highly conserved regions, H1 and H2 [101, 104]. Recent X-ray crystallography studies revealed that the dimerization interface is also located within the head domain, overlapping with H2, whereas the Rab1 binding site was located to the H1 region [104, 105]. In addition, binding sites for the COPI component beta-COP as well as COG2 of the COG complex was also mapped to the head region [104, 105]. Overall, the head region of p115 consists of multi-helical armadillo repeat arranged in right-handed superhelix conformation [105].

Following the head domain, the coiled-coil domain of bovine p115 consists of four separate predicted coiled-coils (CC1-CC4), which cover residues 652-694, 732-766, 786-820, and 849-897, respectively [101]. The proline and glycine rich interruptions between the coiled-coils are predicted to function as flexible hinges, possibly allowing the normally elongated p115 molecule to adopt a bent conformation during its functional cycle [101, 102]. Multiple bent conformations have been observed for p115 by cryo-EM [102]. It was proposed that CC1 may contain an alternative Rab1 binding site that is only exposed upon the binding of other Golgi tethers [106], however, the functional significance of this cryptic site remains unclear. Following the coiled-coil domain is a region of high acidic amino acid content; the extreme C-terminus of p115 forms a very hydrophilic, acidic tail [101]. Other members of the Golgin family, such as GM130 and Giantin, can interact

with this part of the molecule [107-111], though the functional significance of these interactions is controversial [112-114]. [Figure 5]

Various binding partners have been identified for p115. Similar to other Golgins, p115 is a direct effector of Rab GTPase, and seems to be recruited to COPII vesicles through interactions with Rab1 and possibly SNAREs [50, 52]. It has been reported that Rab30 in Drosophila is another potential Rab for p115 [115]. SNAREs that interact with p115 include ER-Golgi SNAREs sec22b, syntaxin 5, membrin and rbet1, as well as Golgi SNAREs Gos28 and GS15, and the neuronal Ykt6 [116]. A SM protein Sly1 also interacts with p115's SNARE-binding domain [116], although the significance of this interaction is unclear.

P115 engages in extensive interactions with many Golgi tethers, among which are Giantin and GM130, two other Golgins. Interactions between p115, GM130 and Giantin appear to be important for maintaining the integrity of Golgi [108, 111], although contradictory evidence has also been reported [113, 114]. Cog2, a COG subunit, is another p115 binding partner. P115 interacts with GBF1, an ADP ribosylation factor (ARF) GEF [117], possibly providing a link between Rab1 and GBF1, which plays a part in the recruitment of COPI coat [118]. A subset of these interactions are depicted in Figure 4A. P115 also directly interacts with the COPI subunit β-COP, which is consistent with p115's role in retrograde ER-Golgi transport and intra-Golgi transport [105]. P115 has multiple phosphorylation sites, and is regulated by a casein kinase II type enzyme during mitosis [109].

P115 is required for a variety of trafficking processes in the cell. The absence of Uso1p/p115 impairs the docking of COPII vesicles [98], as well as the general

early stages of ER-Golgi transport [99]. Depletion of p115 also causes vacuole fragmentation in yeast [94], slows down the stacking of Golgi [56, 57], and disrupts Golgi integrity [119]. In addition to being a Rab1 effector, p115 can affect the recruitment of Rab1 as well [120]. Cleavage of p115 inhibits exocytosis [112]. Also, p115 may regulate Golgi dynamics during mitosis [57]. Taken together with the ubiquitous distribution of p115, these evidences suggest that p115 functions at multiple steps of the early secretory pathway.

Studies of the p115 requirement in the intact animal have also been carried out. P115 knockout (KO) results in embryonic lethality in both mice and Drosophila [114, 121]. Cells from the KO embryos display the characteristic dispersed Golgi morphology seen with p115 knockdown in cultured mammalian cells, suggesting a role of p115 in early embryonic development. Conditional knockout of p115/Uso1p in the C. elegans intestine caused accumulation of transmembrane receptor RME2 in the ER of oocytes, suggesting a block in RME2 transport. In intact animals, p115 depletion seems to affect the trafficking of membrane proteins more than that of soluble proteins [114]. Similar patterns were observed with cultured mammalian cells as well [114, 119, 122]. P115's role in protein sorting at ER exit sites may explain this difference. It was shown that the incorporation of GPI-anchored proteins into ER-derived vesicles requires Uso1p/p115 function [123], thus p115 could have a selective effect on the sorting of certain cargos.

b. P115-SNARE interactions

In early yeast studies, p115 has been implicated to function upstream of SNAREs. Possible interactions between p115 and SNAREs were demonstrated when the lack of p115/Uso1p caused a decrease in the amount of SNARE complexes formed in yeast [96]. There is also evidence suggesting that p115's function is dependent upon its interactions with specific SNAREs [113]. The overexpression of Bet1p or Sec22p, two yeast ER-Golgi SNAREs, suppresses the USO1 deletion in yeast [96]. Later studies identified a group of ER-Golgi SNAREs that potentially interact with p115. When coupled to Neutravidin beads, both CC1 and CC4 were able to retain a subset of ER-Golgi SNAREs (membrin, rSec22p, Bet1p), as well as Golgi SNAREs Ykt6p and GOS-28, from rat liver Golgi extract [116].

In vivo functional replacement of p115 has revealed that the presence of CC1, one of the SNARE-binding domains, is required for maintaining the structure of the Golgi, as expression of CC1-deleted p115 construct failed to rescue the fragmented Golgi phenotype observed with endogenous p115 depletion. Other smaller modifications of CC1 domain also reduced the construct's ability to restore the Golgi ribbons [113]. The same assay also confirmed CC1's requirement for VSV-G transport to cell surface. Taken together, these data imply that CC1-SNARE interactions are indispensable for the function of p115.

In previous co-immunoprecipitation experiments, the CC4 domain, despite its homology to the SNARE motif, appears to have a lower affinity for SNAREs than CC1, which partially contributes to the speculation that CC4-SNARE interactions may not be functionally relevant [116]. More recent studies, however, showed that p115 constructs that lack the CC4 domain act as a dominant-negative on the

structure of Golgi and cargo trafficking [114]. Thus, the CC4 domain might also play a role in the function of p115. Whether this activity of CC4 is SNARE-dependent remains yet unknown.

c. Possible mechanisms of function

P115's involvements in mammalian ER to Golgi transport, intra-Golgi transport, exocytosis, as well as Golgi biogenesis, have all been clearly demonstrated [56, 94-100]. Despite these extensive studies, however, the exact roles of p115 in these processes have yet to be established. One theory is that p115, GM130 and Giantin form string-like structures via their coiled-coil domains, in order to secure vesicles prior to fusion [55, 84]. Also, the close association between p115 and various SNAREs suggests that p115's function is most likely SNARE-related.

The fact that p115 interacts with SNAREs through its SNARE homology domains CC1 and CC4, suggests a different mode of action than the other tethers that bind the SNARE motif. Other SNARE motif-binding tethers, COG component Cog6 and GARP components Vps53 and Vps54, all have SNARE interaction domains localized to the tethers' N-terminal coiled-coils [42], which have no reported SNARE homology. Furthermore, these tethers are capable of binding monomeric SNARE motifs as well as assembled SNARE complexes. On the contrary, if p115 interacts with SNAREs in a similar manner as SNARE-SNARE interactions, it is unlikely that p115 can stay in the SNARE complex after it is assembled, since all the SNARE-motif positions would have been already occupied by cognate SNAREs.

Purified p115 appears to stimulate the assembly of SNARE complexes on Golgi membranes, as well as the assembly of a binary complex by two purified SNAREs [116]. Based on these findings, a 'tweezers' model has been proposed for p115 [Figure 6]. When the opposing membranes are still at a distance, the tail of a p115 dimer splits and the C-terminus of each monomer first binds to a Giantin or GM130 on either membrane, forming a preliminary tether bridge between the vesicle and target membrane. As the membranes come closer, the p115 monomers separate further, with each CC1 domains engaging a SNARE on either side. Still joined at the head, the dimer would draw the SNAREs closer and promote the formation of a SNARE complex [116]. Thus, p115 would act as a SNARE catalyst during fusion, and facilitate the SNAREs to overcome a potential energy barrier between the monomeric state and assembled state [116]. On the other hand, due to the high affinity cognate SNAREs have for each other [14, 40, 124], it is unlikely that the assembly of SNARE complex requires a catalyst [113]. The physiological relevance of p115-mediated SNAREpin assembly, therefore, remains under speculation.

Alternatively, p115 could assemble a membrane-bridging complex by engaging SNAREs on both membranes through its CC1 and CC4 domains simultaneously [125]. The dimer would not need to be split in this model. The CC1 domains of two p115 monomers would interact with either one or two SNAREs on the same membrane, forming a three- or four-helix bundle, while the joined CC4 domains engage SNARE(s) on the opposing membrane. Binding to Rab1 would cause conformational changes in the dimer tail, which would draw the membranes

close and/or 'squeeze' the bound SNAREs together. This model does not exclude the possibility of p115 playing a role as a direct facilitator of SNARE assembly. In addition, by 'capturing' SNAREs through its two SNARE-binding domains, p115 could serve as a SNARE 'fly paper' and increase the local concentration of SNAREs [125].

P115's acidic tail is the binding site for Giantin and GM130. The function of this tail, however, remains a controversial topic. Although the integrity of Golgi seem to depend on the concerted effort of multiple Golgins [54, 59, 61, 108], later studies showed that the removal of p115's tail region does not affect Golgi ribbon structure [113, 114]. It is possible, therefore, that p115 can carry out its function without GM130 or Giantin, at least at certain transport compartments.

The mechanism by which p115 is recruited to membranes and promotes SNARE assembly remains unknown. Previous studies have identified Rab1 as the critical factor of p115 recruitment [50]. However it is not clear whether Rab1 alone is sufficient for maintaining the membrane bound p115 population on COPII vesicles. Later, it was discovered that upon blocking SNARE complex disassembly on *in vitro* budded COPII vesicles with the addition of dominant negative alpha-SNAP, p115 is removed from the vesicle surface, suggesting that p115's recruitment to COPII vesicles is dependent upon unassembled SNAREs in addition to being Rab1 dependent [52, 100]. *In vivo* expression of another SNARE recycling inhibitor, NSF/E329Q, results in decreased p115 membrane association, further suggesting that the disassembly of SNARE complexes is important for maintaining membrane-bound p115 [100].

The above findings imply that p115 preferentially binds to unassembled SNAREs. None of these results, however, eliminates the possibility that alpha-SNAP/NSF competes with p115 for binding to assembled SNAREs. Furthermore, it is presently unclear which ER-Golgi SNAREs are required in p115 recruitment, and whether it is monomeric SNAREs as opposed to SNARE subcomplexes of various stages that p115 binds to. Although unlikely, it is also possible that p115 binds SNAREs to localize to sites of fusion where it performs other functions not directly related to SNAREs.

To further complicate the matter, p115 is present throughout the early secretory pathway, and is required in every step from COPII vesicle budding to maintaining the Golgi stacks. Due to the highly specific protein environments in distinct compartments, it can be assumed that p115 works with a different assortment of cofactors from step to step. It is not clear whether p115 only employs one mechanism of action at all its working sites, or, less likely, that it carries out different functions at different steps in the secretory pathway. It is also unclear whether SNAREs play similar roles at all these steps in regards to p115's function. In addition, due to the fact that p115 is present at more than one compartment and therefore can not contribute to the maintenance of compartment identity simply by its presence, it would be interesting to see if any features of p115's mechanism of action allow it to contribute to the specificity of vesicle targeting.

Therefore, it is essential to further characterize p115-SNARE interactions in detail. It would also be interesting to study p115's role in a controlled in vitro system, in which we could isolate the effects of each domain. Hopefully a structure-

function model for p115 could be derived from a combination of binding and functional studies.

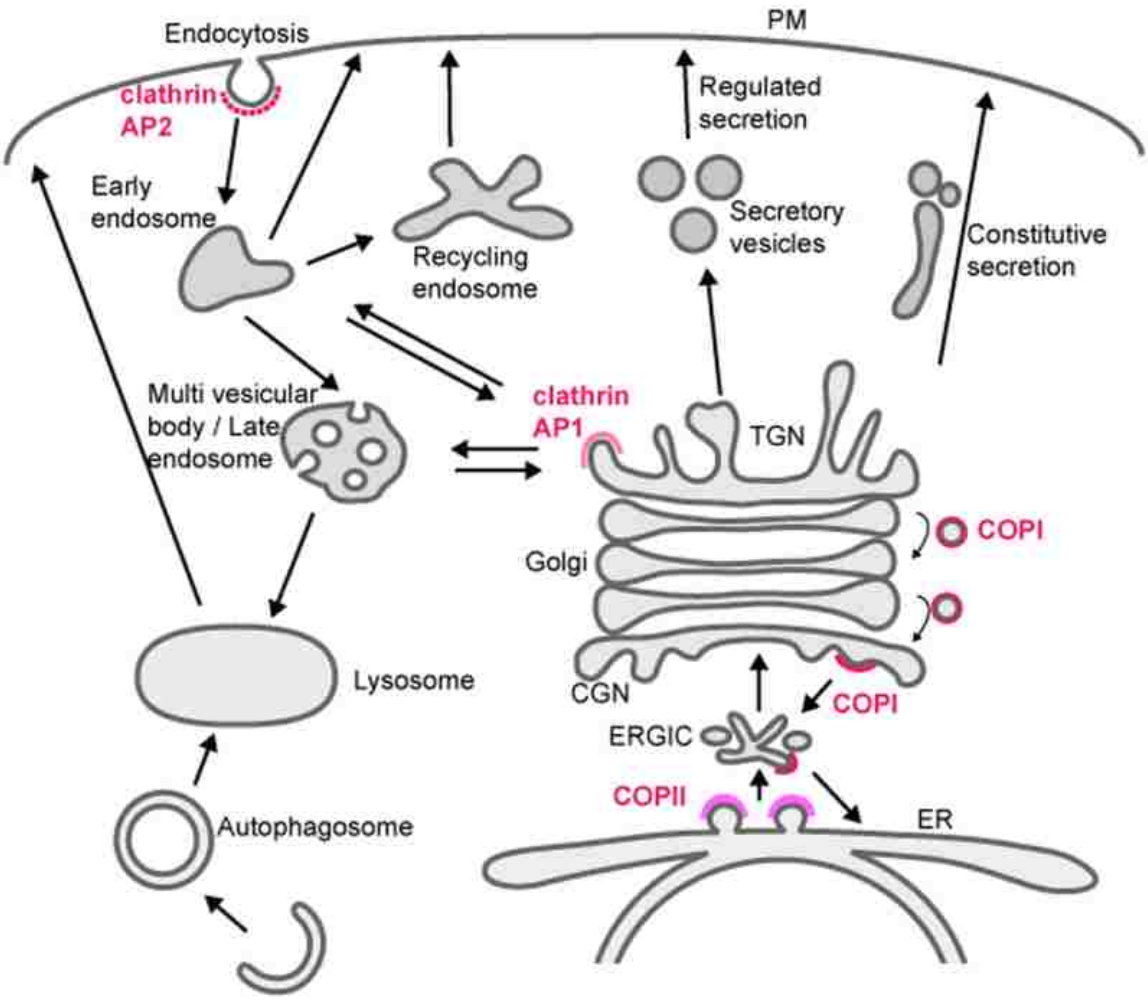

Figure 1. Membrane trafficking pathways in the endomembrane system. ER, endoplasmic reticulum; ERGIC, ER-Golgi intermediate compartment, another term for the vesicular tubular cluster (VTC); CGN, cis-Golgi network; TGN, trans-Golgi network; PM, plasma membrane. Coat proteins are shown in pink.

Adapted with permission from Girard LR, Fiedler TJ, Harris TW, Carvalho F, Antoshechkin I, Han M, Sternberg PW, Stein LD, Chalfie M. WormBook: the online review of Caenorhabditis elegans biology. Nucleic Acids Res 2007;35(Database issue):D472-475.

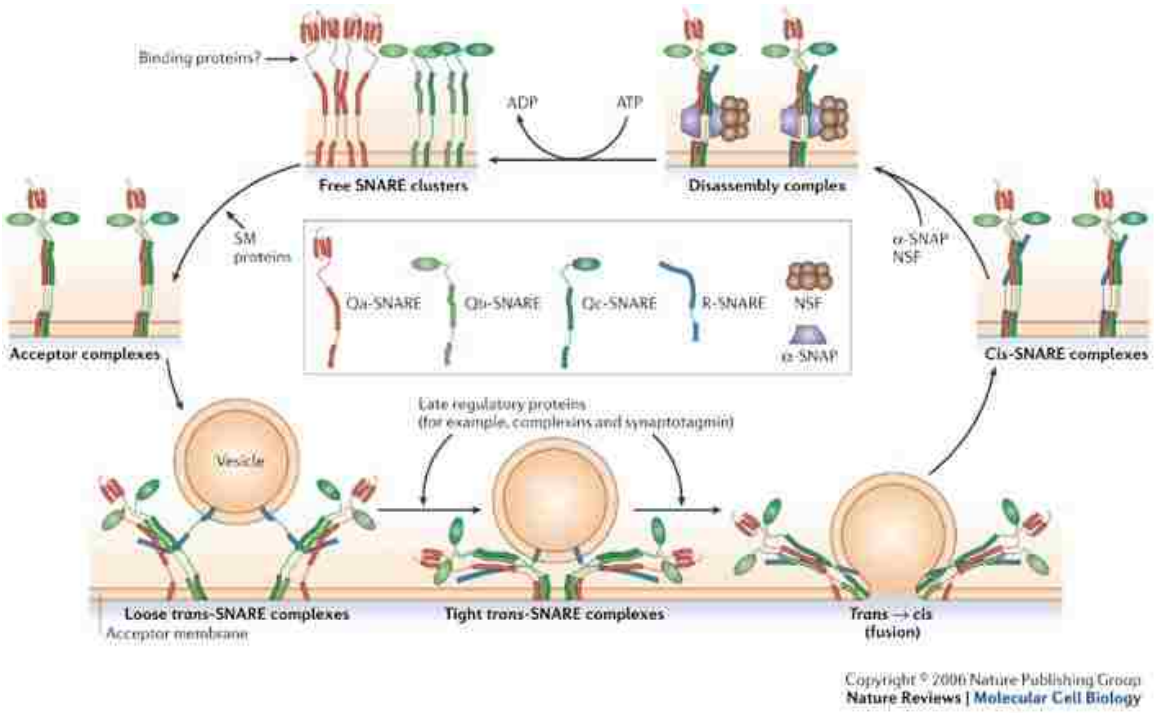

Figure 2: The SNARE mediated membrane fusion and the recycling of SNARE proteins

Adapted with permission from Jahn R, Scheller RH. SNAREs--engines for membrane fusion. Nat Rev Mol Cell Biol 2006;7(9):631-643.

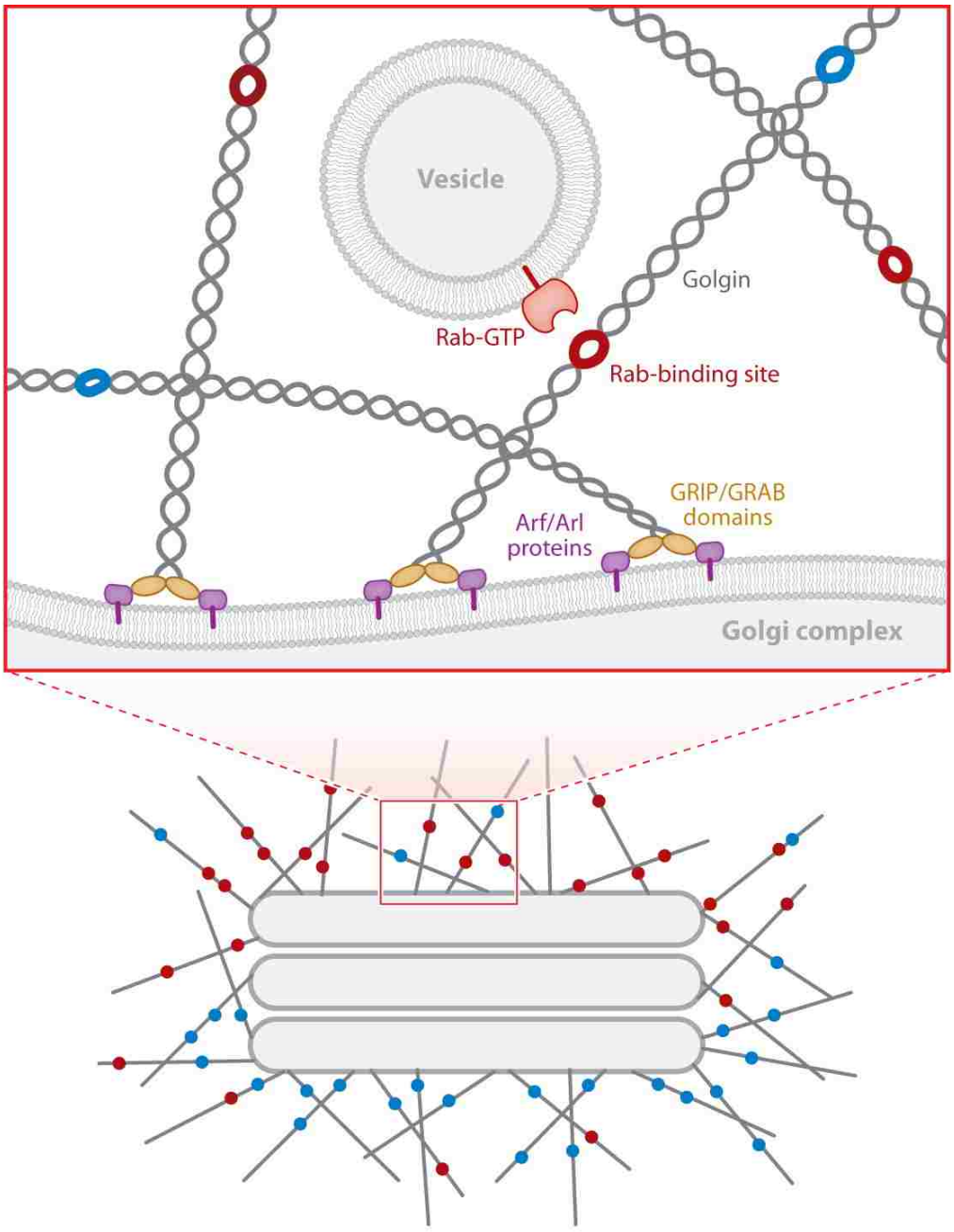

Yu I-M, Hughson FM. 2010.
Annu. Rev. Cell Dev. Biol. 26:137–56

Figure 3. Golgins form fibrous matrix and capture vesicles carrying Rab proteins.

Adapted with permission from Yu IM, Hughson FM. Tethering Factors as Organizers of Intracellular Vesicular Traffic. Annual Review of Cell and Developmental Biology, Vol 26 2010;26:137-156.

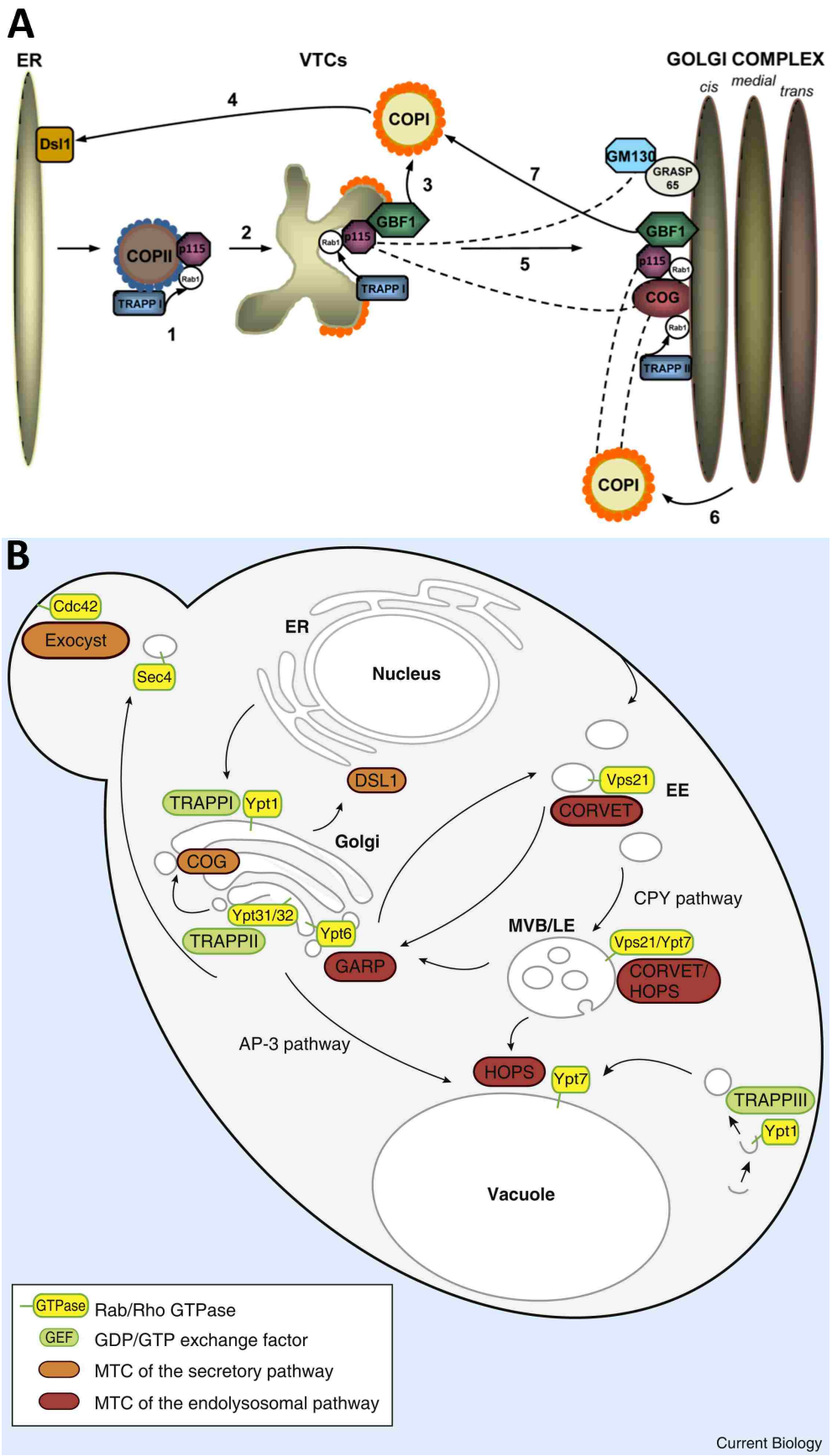
A
ER
VTCs
GOLGI COMPLEX
cis
medial
trans
Dsl1
COPI
COPII
p115
Rab1
TRAPP I
GBF1
GM130
GRASP 65
COG
TRAPP II
1
2
3
4
5
6
7
B
Cdc42
Exocyst
Sec4
ER
Nucleus
DSL1
TRAPPI
Ypt1
Golgi
COG
Ypt31/32
TRAPPII
Ypt6
GARP
Vps21
EE
CORVET
CPY pathway
MVB/LE
Vps21/Ypt7
CORVET/ HOPS
AP-3 pathway
HOPS
Ypt7
TRAPPIII
Ypt1
Vacuole
GTPase Rab/Rho GTPase
GEF GDP/GTP exchange factor
MTC of the secretory pathway
MTC of the endolysosomal pathway
Current Biology

Figure 4. Tethers in the secretory pathway. A. ER-Golgi tethers. Step 1 and 2: P115 is recruited by Rab1 to the COPII vesicles and facilitates fusion. Step 3: Arf GEF GBF1 activates Arf, and recruits COPI coat. Step 4: Dsl1 facilitates COPI fusion. Step 5: P115 facilitates VTCs' fusion with cis-Golgi. Step 6: Newly formed cis-Golgi compartments receive COPI vesicles from more distal Golgi cisterna. Step 7: P115 and GBF1 participate in retrograde transport. B. MTCs and corresponding GTPases. MTCs are shown in orange (secretory pathway) and red (endolysosomal system). Rabs (yeast nomenclature) are indicated in yellow. EE, early endosome; MVB/LE, multivesicular body/late endosome; CPY, carboxypeptidase Y, a vacuole cargo; AP-3, adaptor complex 3 (coatomer).

Adapted with permission from:
A. Sztul E, Lupashin V. Role of vesicle tethering factors in the ER-Golgi membrane traffic. FEBS Lett 2009;583(23):3770-3783.
B. Brocker C, Engelbrecht-Vandre S, Ungermann C. Multisubunit Tethering Complexes and Their Role in Membrane Fusion. Current Biology 2010;20(21):R943-R952.

Tether		Components	Interacting proteins			
			Coats	Small GTPases	SNAREs	Other tethers of relevance
MTCs	HOPS	Pep3 Pep5 VAM6 Vps16 Vps33 Vps41		Ypt7	Vam7 Vam3 Nyv1 Vam2	
	TRAPP I and TRAPP II	Bet3 Bet5 Trs85 Trs65 Trs20 Trs23 Trs31 Trs33 Trs120 Trs130	Sec23 (TRAPPI) γ-COPI (TRAPPII)	Ypt1 Rab1 Ypt31/32		
	COG	COG1 COG2 COG3 COG4 COG5 COG6 COG7 COG8	γ-COPI β-COPI	Ypt1 Ypt6 Rab1 Rab6 Rab30 Rab41	Gos1 Ykt6/Sed5 Sed5 GS28 Syntaxin 5	 P115 GM130
	Dsl1	Dsl1 Tip20 Dsl3	δ-COP α-COP		Sec20/Use1/Ufe1 Syntaxin 18	
	Exocyst	Sec3 Sec5 Sec6 Sec8 Sec10 Sec15 Exo70 Exo84		Sec4 Rho1 Rho3 Cdc42p RalA	Sec9	
	GARP	Vps51 Vps52 Vps53 Vps54		Ypt6	Tlg1 Syntaxin 10 Syntaxin6 Syntaxin16 VAMP4	
Golgins	Giantin	N/A		Rab1, Rab6		p115
	GM130			Rab1, Rab2, Rab33b	Syntaxin 5	p115, Giantin, COG
	P115		β-COP	Rab1, dRab30	GS28, Syntaxin5, membrin, rbet1, sec22b, Ykt6, GS15	Giantin, GM130, COG2

Table 1. Golgi tethering proteins and protein complexes

Adapted with permission from Table 1, Sztul E, Lupashin V. Role of vesicle tethering factors in the ER-Golgi membrane traffic. FEBS Lett 2009;583(23):3770-3783.

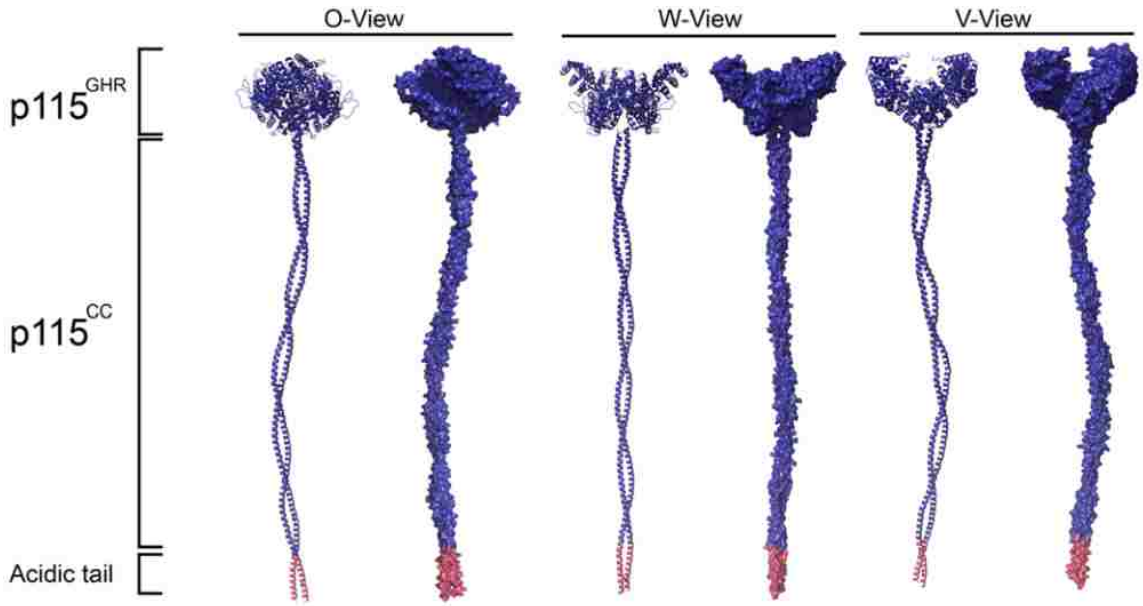

Figure 5. Model of the overall fold of the full-length p115. Surface and cartoon representations of a model of the full-length p115 generated by manually fitting a coiled-coil of appropriate length to the C-termini of $p115^{GHR}$ in the crystallographic dimer. $P115^{GHR}$: p115 globular head region; $p115^{CC}$: p115 coiled-coil region.

Adapted with permission from Striegl H, Roske Y, Kummel D, Heinemann U. Unusual armadillo fold in the human general vesicular transport factor p115. PLoS One 2009;4(2):e4656.

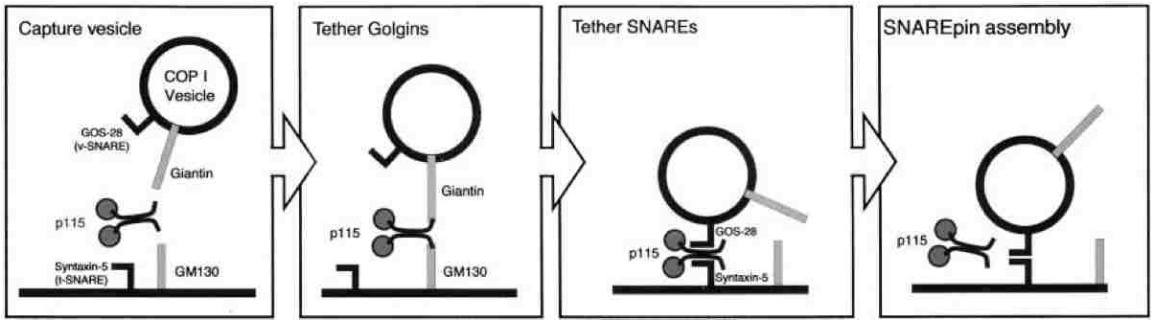

Figure 6: A sequence of events in the 'tweezers' model of p115 function.

Adapted with permission from Shorter J, Beard MB, Seemann J, Dirac-Svejstrup AB, Warren G. Sequential tethering of Golgins and catalysis of SNAREpin assembly by the vesicle-tethering protein p115. J Cell Biol 2002;157(1):45-62.

Chapter II: Methods

A. Protein Purification

Recombinant SNARE proteins were expressed and purified as previously described [29]. Hexahistidine-tagged full-length bovine p115 was expressed in E. coli strain NM522 using a pQE9 construct obtained from the Lowe lab [84]. Bacteria cultures were grown at 37°C to an A_{600} of 0.4, before induction with 1 mM isopropyl-1-thio-β-D-galactopyranoside at the same temperature for 2-3 hours. Bacteria were pelleted and resuspended in French Press buffer (50 mM Tris, pH 8.0, 0.1 M NaCl, 1 mM EDTA, 0.05% Tween 20, 2 μg/ml leupeptin, 4 μg/ml aprotinin, 1 μg/ml pepstatin A, and 1 mM phenylmethylsulfonyl fluoride). After 2 rounds of French Press, cell lysates were centrifuged at 20,000 x g for 20 minutes, the supernatant was then collected and centrifuged again at 100,000 x g for 45 minutes. Supernatant from the second centrifigation was passed through a Ni-NTA column equilibrated with 50 mM Tris, pH 8.0, 0.3 M NaCl, 0.05% Tween 20, and 0.025 M imidazole, and eluted with the same buffer containing a 0.025-0.25 M gradient of imidazole. Purified His-tagged p115 was dialyzed into protease inhibitors (1 mM DTT, 2 μg/ml leupeptin, 4 μg/ml aprotinin, and 1 μg/ml pepstatin A) supplemented Buffer A (20 mM Hepes, pH 7.2, 0.15 M KCl, 2 mM EDTA, 5% glycerol), and quantitated according to A_{280}. Sec22b N-terminal domain was present as a major degradation product in the sec22b preparation, and was separated from the full-length protein by gel filtration. Hexahistidine-tagged membrane N-terminal domain and hexahistidine-tagged Ykt6 N-terminal domain were expressed using pQE9 constructs and purified in the same way as full-length sec22b.

For the in vitro tethering and fusion assay, Ni-NTA purified p115 was further purified on an ion exchange column (FPLC-Mono Q, Amersham Pharmacia Biotech). The column was washed abundantly with running buffer (20 mM Tris, 1mM EGTA, pH 7.6). After loading p115, the column was washed with 15 ml running buffer, then eluted with the same buffer containing a 0-1 M gradient of KCl. Purified p115 was dialyzed into 25 mM Hepes, 125 mM potassium acetate, pH 7.2.

p115 from rat liver cytosol was partially purified by two procedures. The first procedure essentially followed [95], with minor modifications; this generated a MonoQ fraction with a simple protein pattern in which p115 is a major band by SDS gel and Coommassie staining. A second procedure involved ammonium sulfate fractionation as in Barroso et al., followed directly by Superdex 200 gel filtration. The peak Superdex 200 fraction was quite complex, but was enriched for p115 by 18-fold relative to cytosol.

B. Gel Filtration Chromatography

Individual purified recombinant SNAREs were either loaded onto a gel filtration column alone, or loaded after incubation with p115. Eluted fractions were collected, acetone precipitated and analyzed by SDS-PAGE and Western blotting [Figure 7].

The gel filtration column use for this study is a pre-packaged 24-ml Superdex 200 (Amersham Pharmacia Biotech). By comparing the elution of the SNARE/p115 mixture, and the SNARE only elution, we will be able to determine whether the SNARE in question has entered into a complex with p115, indicated by a shift of the

elution peak. It is worth noting that due to p115's elongated shape, it is eluted as a ~700kD protein. This is normal for the p115 dimer, as described in literature [56].

For the p115-monomeric SNARE binding assay [Figure 12A-I], approximately 20 μg of each full-length SNARE protein or NT domain was incubated with or without ~1.3 μM of p115 in Buffer A supplemented with 0.1 % Triton X-100, in a reaction volume of 300 μl. After an overnight incubation, 250 μl of each protein mix was fractionated on the gel filtration column equilibrated in Buffer A containing 0.5 mg/ml BSA and 0.1% Triton X-100. Fractions were acetone-precipitated and subjected to SDS-PAGE and Western analysis with anti-SNARE antibodies.

For the SNARE monomer vs. complex binding assay [Figure 14], all reactions were conducted in the same buffer used in other gel filtration experiments. Purified recombinant rbet1, syntaxin 5, and membrin were incubated together on ice for 48 hrs, before loading onto 5–30% glycerol gradients run in Buffer A supplemented with 0.1% Triton X-100, then centrifuged at 200,000 x g for 24 hrs in a Beckman MLS-50 rotor. Rbet1 alone was also subjected to velocity sedimentation under the same conditions. Fractions from both gradients were analyzed and quantitated with anti-rbet1 Western analysis, complex and monomer fractions were each pooled and dialyzed into Buffer A containing 0.1% Triton X-100.

In the SNARE complex assembly assay [Figure 17], for the instantaneous effects of p115 [Figure 17 A and C, left panel], 50 μl of purified recombinant syntaxin 5, membrin, rbet1, and sec22b were incubated together on ice for 4 hrs, in the presence or absence of 0.9 μM of p115. The reactions were subjected to gel filtration as described above. The fractions were acetone-precipitated, dissolved in sample

buffer and analyzed with Western blotting for sec22b.

For the chaperone effects studies [Figure 17B and C, right panel], 50 µl of purified recombinant sec22b was incubated with p115 overnight on ice, before the addition of syntaxin 5, membrin, and rbet1. The final p115 concentration in the reaction mix was 0.9 µM. For the control reaction, sec22b was incubated alone on ice overnight, before the addition of other SNAREs and 0.9 µM of p115. Both reactions were incubated on ice for 4 hrs, then subjected to gel filtration, SDS-PAGE, and Western analysis for sec22b as described above.

C. Bead Binding Assay

GST tagged recombinant SNAREs were fixed onto glutathione-Sepharose beads, and incubated with p115. The beads were then washed and analyzed by SDS-PAGE and Western blotting. Retention of p115 or, in the case of the p115 displacement experiment, the amount of p115 in solution was compared to the GST control beads.

For the SNARE-p115 binary binding experiments [Figures 8 and 13], 100 µl of 50% glutathione-Sepharose beads containing 0.5 mg/ml membrin, rbet1, or GST was each incubated with 20 nM and 60 nM of p115, respectively, in the presence of Buffer A containing 1 mg/ml BSA and 0.1% Triton X-100. Reaction volume was 200 µl. All reactions were incubated at 4°C overnight with agitation. Beads were then pelleted and washed with 3 x 1 ml of the same reaction buffer, after which 50 µl of SDS-PAGE sample buffer was added to each pellet prior to SDS-PAGE and Western analysis. For bead binding assays shown in Figure 20, only 20 µl of beads were used

per 200 µl reaction, but the other parameters were similar.

For the p115 displacement experiment [Figures 9 and 15], reactions were conducted in the same buffer as the binary binding experiments. 100 µl of 50% glutathione-Sepharose beads containing 0.5 mg/ml rbet1 or GST was incubated with 600 nM p115 at 4°C overnight with agitation. The next day, after washing the beads with 3 x 1ml of reaction buffer, 0.025, 0.05, or 0.075 mg/ml of membrin or BSA was added to the reactions. All reactions were then incubated at 4°C for 4 hrs with agitation. The supernatants were collected and supplemented with equal volume of sample buffer, before subjected to SDS-PAGE and Western analysis for p115.

D. *In vitro* Budding, Tethering and Fusion Assays

Our lab has developed a method to generate and study the fusion and tethering of COPII coated compartments *in vitro* [Figure 10]. This assay utilizes the vesicular stomatitis virus glycoprotein (VSV-G) ts045 as a model cargo. Normal rat kidney cells were either transfected with myc-VSV-G DNA, or infected with VSV then pulse radiolabeled. Following an incubation at 40°C that allows VSV-G to accumulate in the ER, both populations of cells were permeabilized and incubated in the presence of rat liver cytosol, ATP regenerating system, and buffer, thus producing two distinctly labeled, fusogenic COPII vesicle populations.

Due to an equilibrium between VSV-G trimers and monomers [126], fusion of the differently labeled vesicles will result in a heterotrimer containing both the myc-labeled VSV-G monomer and the S^{35} labeled VSV-G* monomer. This kind of heterotrimer can only arise from fusion, but not tethering of the vesicles. This

property of the VSV-G trimer allows us to study the events of fusion and tethering separately in our in vitro assay.

NRK cells were transfected with myc-VSV-G DNA. After 24 hrs, cells were infected with vaccinia virus, followed by a 5 hr incubation at 40°C. The cells were then permeabilized by scraping and suspended in 25/125 buffer. Myc-labeled vesicles were produced in a buffer consisting of 75 µl of the cell suspension, 96 µl of water, 65 µl of 25/125 buffer, 15 µl of 0.1 M magnesium acetate, 30 µl of ATP-regenerating system, 9 µl of 1 M HEPES, pH 7.2, 60 µl of Ca/EGTA buffer (20 mM HEPES, pH 7.2, 1.8 mM $CaCl_2$, and 5 mM EGTA), and 150 µl of rat liver cytosol dialyzed in 25/125 buffer. After incubation at 32°C for 30 minutes, cells were removed from the reactions by centrifigation. 160 µl of recombinant rbet1 (~2.5 µg) in Buffer A, 160 µl of Buffer A, or 160 µl of 25/125 buffer (positive control) was then added to the vesicles. Reactions were incubated on ice for 20 minutes prior to another 1 hr incubation at 32°C, after which vesicles were immunoisolated with 5 µg of anti-myc mAb, and subjected to SDS-PAGE and Western analysis.

COPII vesicle co-isolation and heterotrimerization assays were also carried out as previously described. Two distinctly labeled COPII vesicle populations were generated for these assays. Myc-VSV-G-containing vesicles were prepared as described above. To prepare the ^{35}S-labeled vesicles, NRK cells were transfected with vesicular stomatitis virus strain ts045 and incubated at 32°C for 4 hrs, before labeling with 500 µCi of ^{35}S-cysteine/methionine at 40°C, in a cysteine/methionine-free medium. Cells were then permeabilized and suspended in 25/125 buffer. Both types of vesicles were produced in a reaction mix consists of 337.5 µl of either cell

suspension, 432 µl of water, 67.5 µl of 0.1 M magnesium acetate, 135 µl of ATP-regenerating system, 40.5 µl of 1 M HEPES, pH 7.2, 270 µl of Ca/EGTA buffer, and 675 µl of rat liver cytosol (either untreated, mock-depleted, or p115-depleted, all dialyzed in 25/125 buffer). Supernatants containing COPII vesicles were collected by centrifigation. 72.5 µl of myc-VSV-G vesicle suspension and 72.5 µl of ^{35}S-VSV-G vesicle suspension were added to each reaction tube. For certain reactions, recombinant p115 dialyzed in 25/125 was also added. The final volume of all reactions was brought up to 200 µl with 25/125 buffer. Reacion tubes were first incubated on ice for 20 minutes, then shifted to a 32°C water bath and incubated for another 1 hr.

Treatments for fusion versus tethering assays differ from this point on. For the tethering/co-isolation assay, the reactions were chilled and centrifuged at 20,000 x g for 5 minutes to remove large vesicles, then immunoisolated with 5 µg of biotinylated anti-myc mAb and 10 µl 50% streptavidin-Sepharose (GE Healthcare). The isolates were dissolved in sample buffer, run on 12% SDS-PAGE gels, and transferred to nitrocellulose membrane. The amount of myc-VSV-G in each isolate was quantitated by Western analysis. The membrane was then dried and analyzed by phosphorimaging. Amounts of ^{35}S were measured, and normalized based on the myc-VSV-G level, which reflects the amount of vesicle present. For the vesicle fusion assay, 2% Triton X-100 was added to the reactions following the 1 hr incubation at 32°C. Reactions were then incubated with agitation at 4°C for 20 minutes, before centrifugation at 100,000 × g for 30 min. Immunoisolation and analysis were performed on the supernatants as described for the tethering assay.

To generate p115-depleted cytosol, Pansorbin beads (Calbiochem) were washed five times with 50 x volume 25/125 buffer (25 mM Hepes, 125 mM potassium acetate, pH 7.2), and re-suspended at a concentration of 10%. Rat liver cytosol was dialyzed into 25/125 buffer, then supplemented with 0.05 x volume of affinity-purified rabbit anti-p115 (see below) and incubated at 4°C for 2 hrs. Immediately after the incubation, Pansorbin suspension was added to the cytosol at a concentration of 0.06 x volume. The mixture was incubated with agitation at 4°C for 15 minutes, before centrifugation at 20,000 x g. The supernatant was centrifuged again at 20,000 x g. Supernatant from the second centrifugation was then collected. In addition, a mock-depleted RLC was produced using identical methods and non-immune rabbit IgG.

E. Endoglycosidase H Acquisition Assay

During ER-Golgi transport, a fourteen-subunit oligosaccharide linked to a cargo protein is modified at the Golgi by Golgi alpha-mannosidase II, and the protein acquires Endo H resistance by this process. Therefore, the percentage of Endo H resistant population of a select cargo reflects the efficiency of ER-Golgi transport of the glycoprotein cargo [127].

For the ER-Golgi transport assay, to reduce the p115 'background', NRK cells were electroporated with p115 siRNA (Ambion, Silencer Select; 5'-CUAUUGACGCAACAGGUAAtt-3') twice over five days prior to assays. NRK cells were then infected with VSV-G, shifted to 40°C and pulse-radiolabeled with ^{35}S-labeled amino acids. The cells were permeabilized as describe above in the fusion assay, and

reconstituted with rat liver cytosol, various other soluble proteins, and an ATP-regenerating system, then incubated at 32°C to allow ER to Golgi transport to occur. Incubated semi-intact cells were dissolved in detergent and proteins were digested with or without endoglycosidase H. The endoglycosidase H-resistant VSV-G in each sample was determined following gel electrophoresis and autoradiography. Percent endoglycosidase H resistance of VSV-G, the measure of ER to Golgi transport, was defined as the intensity of the endoglycosidase H resistant band divided by the sum of the resistant and sensitive bands x 100%.

F. P115 Depletion and Overexpression in HeLa Cells

For the overexpression of p115, HeLa cells were transfected with full-length myc-tagged p115. For the depletion of p115 and subsequent rescue, Hela cells were transfected with anti-human p115 siRNA for 3 days and then transfected with myc-tagged rat full-length p115. SiRNA and construct design, transfection, and immunofluorescence microscopy were all performed as previously described [114].

G. Antibody Production

Hexahistidine-tagged rat p115 construct was expressed in E. coli with pET-21b vector. Cultures were grown at 37°C to an A_{600} of 0.5, before induction with 0.5 mM isopropyl-1-thio-β-D-galactopyranoside at the same temperature for 3 hours. Harvested cells were subjected to two rounds of French Press and centrifuged at 20,000 x g for 20 minutes. The supernatant was then collected and centrifuged again at 100,000 x g for 45 minutes. Pellets from the second centrifigation were collected

and dissolved in sample buffer and loaded onto SDS-PAGE gels. Gels were stained with 0.1% Commassie in water, and the resolved p115 bands were excised from the gel and subjected to electroelution in 25 mM Tris, 191 mM glycine, 0.1% SDS, and 1 mM DTT. The eluted protein solution was concentrated and injected subcutaneously into a rabbit using Freund's adjuvant. Collected sera were supplemented with equal volume of 10 mM Tris, pH 7.5, filtered with syringe filter, and passed through a CNBr-Sepharose column conjugated with GST as nonspecific control. The flowthrough was then loaded onto another CNBr-Sepharose column conjugated with rat p115. After sample loading, columns were washed with 3 x 5ml of 10 mM Tris, pH 7.5, then washed with the same buffer containing 0.5M NaCl, once again with 10 mM Tris, pH 7.5, and finally eluted with 0.1M glycine, pH 2.5. Fractions were neutralized with 2M Tris, pH 8.0, and quantitated at A_{280}. Peak fractions were pooled and dialyzed into 25/125 buffer.

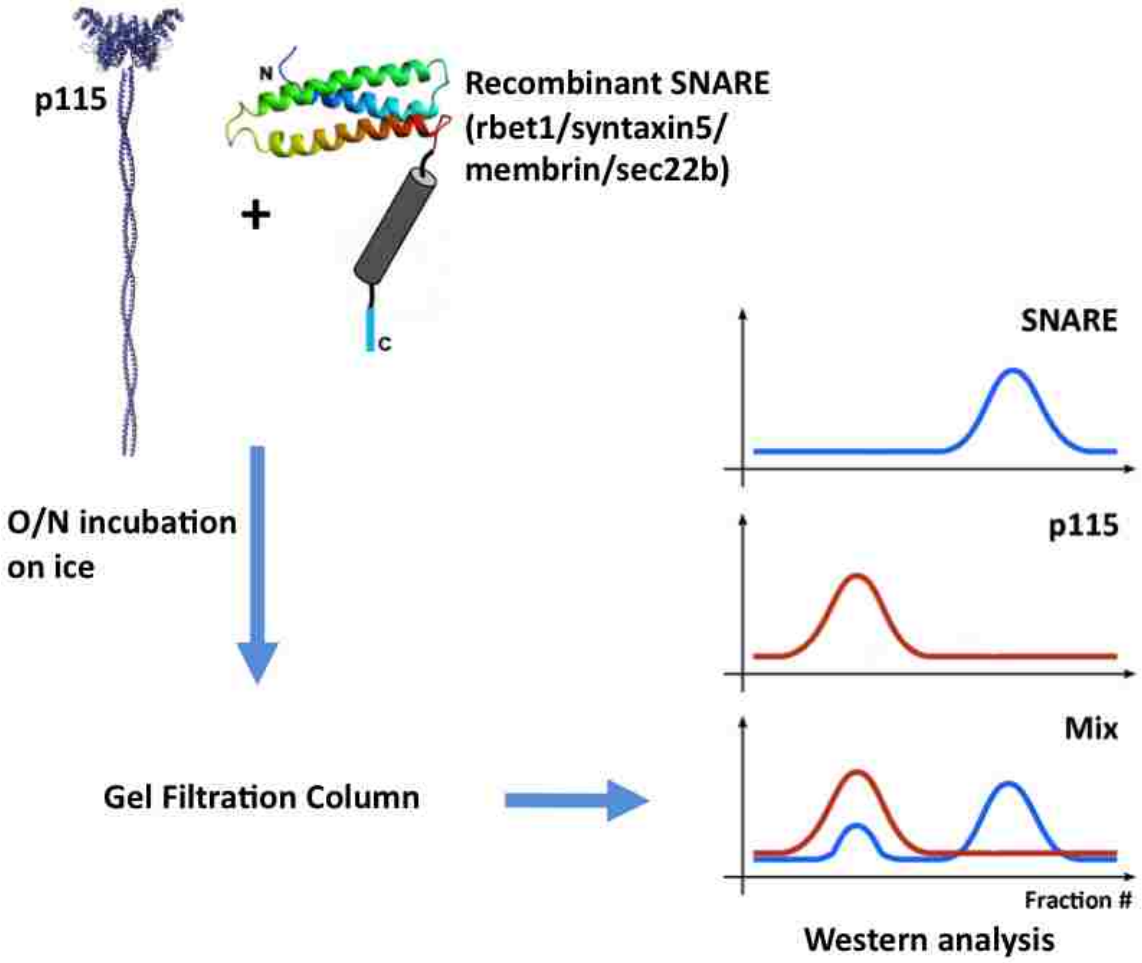

Figure 7: General procedure of the gel filtration assay.

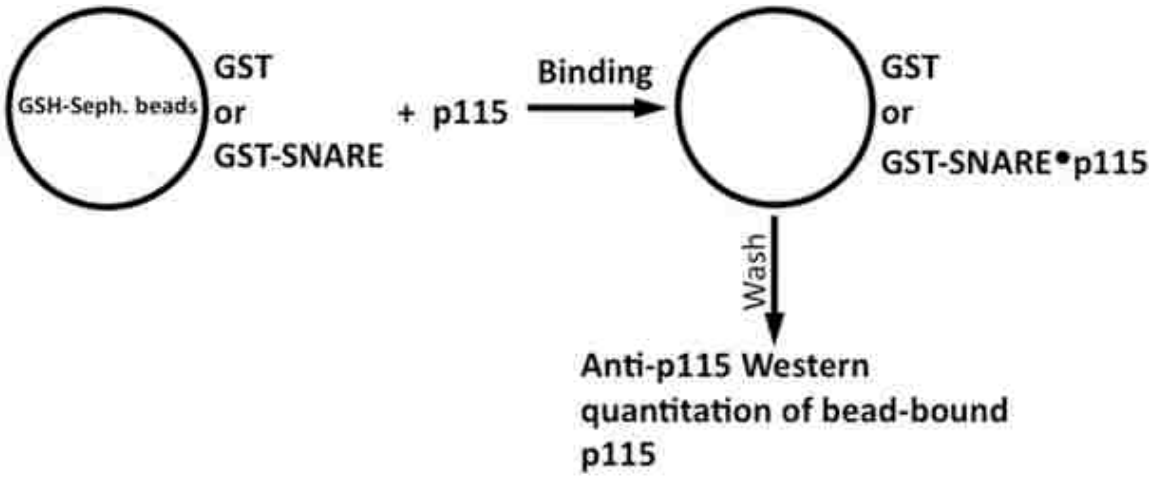

Figure 8: SNARE-p115 binary bead binding experiment.

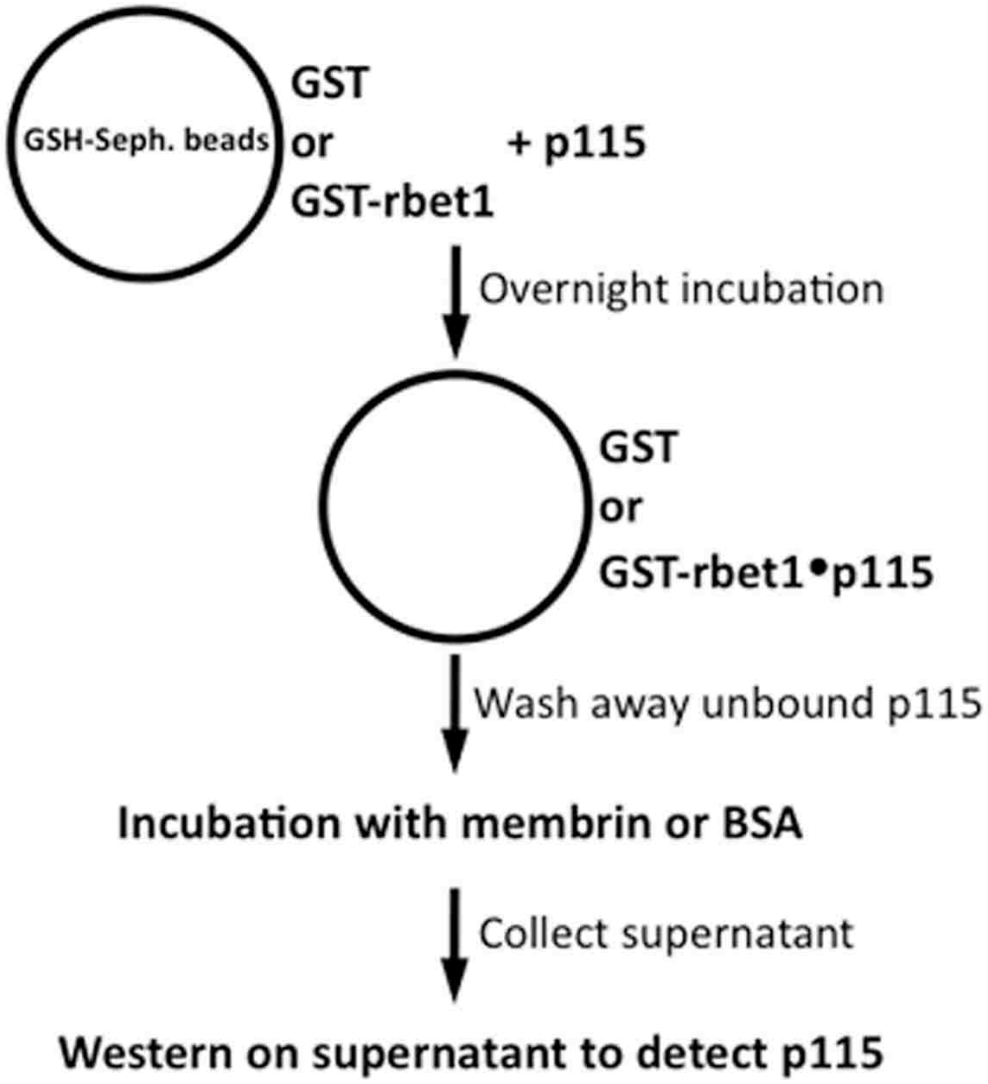

Figure 9: P115 displacement bead binding experiment.

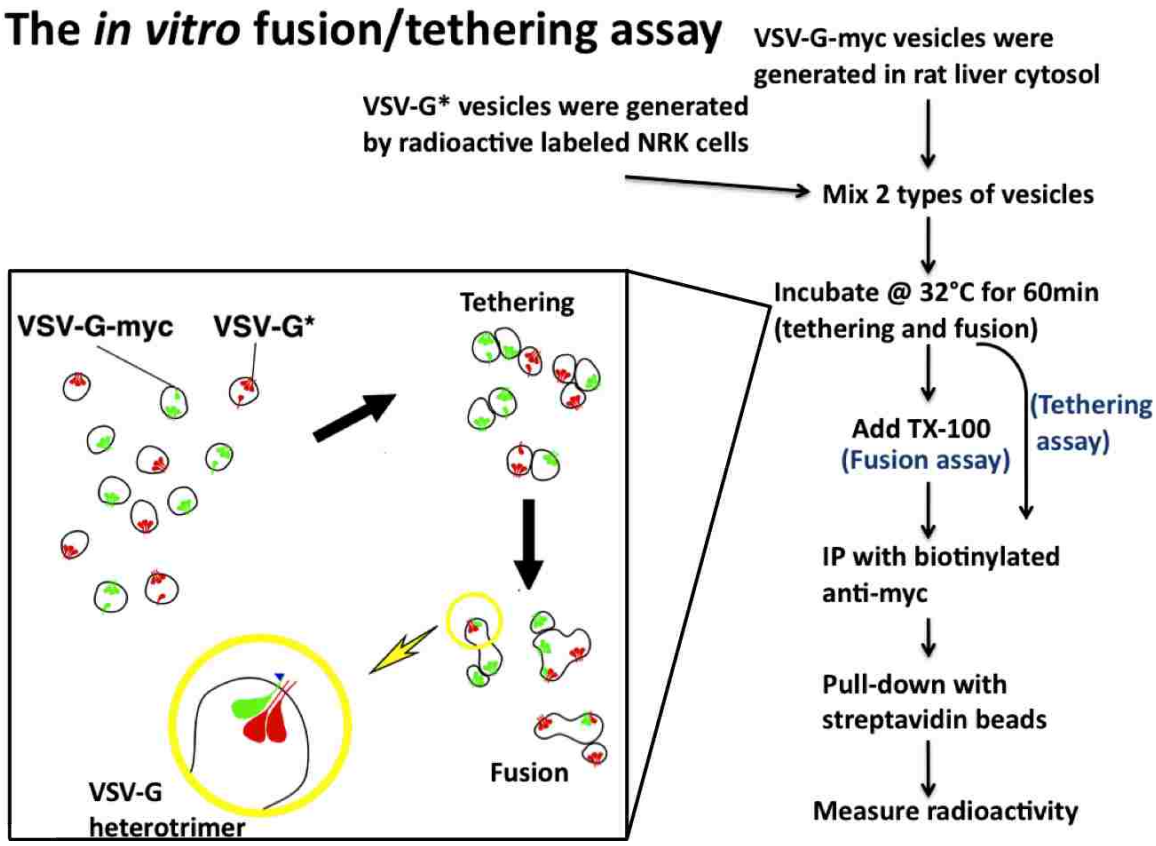

Figure 10: The in vitro COPII vesicle budding, tethering, and fusion system.

Chapter III. P115 Selectively Binds Monomeric SNAREs

A. P115's Interactions with Individual ER-Golgi SNAREs

Previous studies demonstrated that p115 coprecipitates with syntaxin 5, membrin, bet1p (rbet1), and sec22b [50, 116], yet direct and specific binding interactions between p115 and these SNAREs, individually and as subcomplexes, have not been explored. Detailed knowledge of these interactions is key to understanding the p115 mechanism of action. To study directly p115's interactions with SNAREs, we first prepared soluble ER-Golgi SNARE proteins. Cytoplasmic domains of rat ER/Golgi SNAREs sec22b (residues 2-196), syntaxin 5 (the shorter isoform, representing residues 55-333 of the longer isoform), and rbet1 (residues 1-95) were expressed in E. coli and purified using column chromatography as described before [29]. We were unable to express the cytoplasmic domain of membrin in E. coli, but a full-length membrin construct (residues 2-212) was well-expressed, soluble in mild detergent and active in binding studies. His6-tagged full-length bovine p115 was also well expressed and freely soluble, and was purified by column chromatography. This p115 preparation has been previously shown to be active in SNARE interaction assays [84]. Figure 11 shows an SDS gel analysis of the protein preparations typically used in these studies.

Our binary binding studies utilized a gel filtration assay that only detects stable complexes formed in solution. Purified p115 was passed through a Superdex 200 column. Due to its elongated shape, the peak of p115 elution was in fraction 10 (Figure 12A), at a predicted size of 700 kD, much larger than the expected 230 kD dimer, as shown previously [56]. This unusual feature of p115 made a gel filtration

SNARE binding assay feasible since the p115 elution did not overlap with SNARE complexes or homo-oligomers. Next, soluble syntaxin 5, membrin, rbet1, and sec22b were passed through the Superdex column separately, fractions were collected and analyzed by Western blotting. Rbet1, sec22b, syntaxin 5 and membrin were eluted in fractions 28-34, 26-36, 18-30, and 16-30, respectively (Figure 12B-E, top panels, slightly different fractions are shown to optimize display of each protein). The SNAREs were then each incubated separately with p115 overnight on ice, the reactions were subjected to gel filtration and analyzed by Western using anti-SNARE antibody. The elution of each mixed incubation (Figure 12B-E, bottom panels) was compared to the SNARE-only elution (top panels). In the presence of p115, a significant portion of both rbet1 and sec22b shifted to higher molecular weight fractions, indicating the formation of a complex. Furthermore, the elution peaks of the complexes overlapped the p115 peak, suggesting the presence of p115 in these complexes. Since the p115/SNARE complexes overlapped the void volume of the column, especially in the case of sec22b (part C), we independently verified the presence of freely soluble p115-sec22b complexes by centrifuging the co-incubated proteins at 100,000 x g to remove high molecular weight aggregates followed immediately by co-immunoprecipitation of the two proteins using anti-p115 antibody (Figure 12J).

B. SNARE Motif is the Binding Site for P115

Structurally, a typical SNARE consists of an N-terminal domain, a SNARE motif, and a membrane anchor [12]. Most SNARE-binding tethering complexes such as the

Dsl1 complex, Golgi-associated retrograde protein (GARP) complex and homotypic vacuole fusion and protein sorting (HOPS) complex, primarily interact with the N-terminal domain of SNAREs [70, 77, 78, 128, 129], whereas the conserved oligomeric Golgi (COG) complex preferentially interacts with the SNARE motif of Sed5p [87]. The CC1 and CC4 domains of p115 share weak sequence homology to the SNARE motif [116, 130], and it has been demonstrated that p115 interacts with SNAREs through these two domains [113, 114, 116]. The binding site for p115 on a SNARE has not been mapped before, but we expected that p115 binds the SNARE motif through coiled-coil interactions, similarly to SNARE-SNARE binding. As one demonstration of this principle, rbet1 is a SNARE that lacks the N-terminal domain, meaning that the cytoplasmic portion of rbet1 (residues 1-95) employed in our binding studies consists solely of the rbet1 SNARE motif. Since p115 and the SNARE motif of rbet1 formed a stable complex that can be resolved by gel filtration (Figure 12B), the SNARE motif must be the binding site for p115.

However, these results do not exclude the possibility that p115 can also interact with a SNARE's N-terminal domain. Sec22b has an unusual N-terminal structure composed of a β-sheet and several α-helices termed the longin domain [32]. Similar structures of other SNAREs have been reported to bind SNARE motifs and exert regulatory effects on SNARE activities [131-133] and localization [34]. The longin domain of sec22b contains two potential binding grooves for the SNARE motif, although intramolecular binding has not been clearly demonstrated. To test possible interactions between p115 and the sec22b longin domain, we expressed and purified the N-terminal longin domain of sec22b. We did not detect any binding

between the sec22b longin domain and p115 using the gel filtration assay (Figure 12G), which provides additional support that p115 interacts with the SNARE motif. In addition, we also purified the N-terminal regions of membrin, that possesses a three-helix N-terminal domain [134, 135], and Ykt6, another ER-Golgi SNARE that possesses a longin domain that has been shown to interact with SNARE motifs [34, 131], and tested their binding to p115. No binding was detected between p115 and either construct (Figure 12H, I).

C. P115 Interacts with Monomeric SNAREs, but not SNARE Complexes

We noted that membrin and syntaxin 5, two SNAREs that have been shown to interact with p115 using a bead-binding format [50, 116], did not form stable complexes with p115 under our binding conditions (Figure 12, D and E.). One obvious possibility is that the syntaxin 5 and membrin N-terminal domains bound their respective SNARE motifs, precluding p115 access. The syntaxin 5 N-terminal domain has been shown to reduce other SNARE binding [29]. To test for potential interference by the syntaxin 5 N-terminal domain, a highly active construct consisting of only the SNARE motif of syntaxin 5 (residues 252-333) was generated by thrombin cleavage of the cytoplasmic domain (residues 55-333), and purified by velocity sedimentation. This fragment of syntaxin 5 was demonstrated to be at least an order of magnitude more efficient in SNARE complex formation than the full cytoplasmic form [29]. However, when we used the truncated construct in gel filtration studies, we were unable to detect binding between p115 and the syntaxin 5 SNARE motif (Figure 12F).

Perhaps relevant to their lack of binding, we also noticed that both membrin and syntaxin 5 eluted in fractions in the 150-200 kD range, much larger than their expected monomer molecular weights of 25 and 34 kD, respectively. For reference, the syntaxin 5-membrin-rbet1-sec22b 1:1:1:1 complex in this system elutes in fraction 17 with a calibrated molecular weight of ~300 kD [29]. Apparently, under our purification conditions, syntaxin 5 and membrin form homo-oligomeric coiled-coils in solution. Furthermore, p115's binding could have been prevented by this oligomerization.

These results left two possibilities to explain the lack of p115 binding to syntaxin 5 and membrin; 1) p115 does not form stable complexes with SNARE oligomers or 2) p115 is selective for binding certain SNAREs, and does not interact with syntaxin 5 and membrin. However the latter possibility seems unlikely since interactions between p115, syntaxin 5, and membrin have been observed [50, 116]. More likely, our particular protein preparations and/or gel filtration binding assay are able to detect a binding preference for monomeric SNAREs that had not been apparent before.

To further analyze possible interactions between p115 and membrin, and to understand the basis for the potential discrepancy with the literature, GST-tagged full-length membrin was immobilized on Glutathione-Sepharose beads, along with GST or GST-rbet1 for negative and positive controls, respectively. These beads were then incubated with p115, washed, and the levels of bound p115 were analyzed by SDS-PAGE and immunoblotting (Figure 8). By using this bead-binding assay, we were able to demonstrate specific binding between p115 and membrin beads

(Figure 13). However, unlike GST-rbet1, GST-membrin bound only at higher p115 concentrations at which nonspecific binding was also evident. Since a higher affinity interaction is more likely to be solution-stable, this likely explains why membrin and syntaxin 5 failed to produce complexes in the gel filtration assay, and suggests that the discrepancy we saw was due to different experimental conditions.

In summary, p115 bound stably to rbet1 and sec22b in solution, but did not form stable complexes with membrin or syntaxin 5 (Figure 12). The low affinity interactions observed with membrin in the bead format, together with the fact that p115 did not stably interact with the highly active syntaxin 5 SNARE motif led us to hypothesize that oligomerization was the main reason for p115's apparent selectivity in the gel filtration binding assay. If this is true, then the formation of a hetero-oligomeric SNARE complex, which is structurally even more robust than SNARE homo-oligomers, is predicted to also block the binding of p115.

Since the formation of a SNARE complex does not involve the SNARE N-terminal domains, it is not surprising that tethers associating with SNARE N-terminal domains can remain bound to the SNARE complex after its completion [70]. However, it is harder to imagine p115, which interacts with SNARE motifs, not being displaced after the SNARE motifs assemble into a four-helix-bundle. Studies have demonstrated that despite its involvement in SNARE assembly, p115 can be washed off with high salt from formed SNARE complexes, indicating that p115 is not integrated into these complexes [116]. P115/Uso1p-facilitated SNARE assembly yields SNARE complexes lacking p115 [96, 116]. Furthermore, blocking the recycling of SNAREs decreases the amount of membrane-associated p115 [52],

suggesting SNARE complexes cannot recruit p115 as efficiently as SNAREs in monomeric form.

To test whether p115 can interact with SNARE complexes, we performed a solution binding study using rbet1 in its hetero-oligomeric vs. its monomeric state. Recombinant rbet1, syntaxin 5 and membrin were incubated together prior to fractionation by velocity gradient sedimentation. The presence of rbet1-containing SNARE complexes in fraction 7 was detected by anti-rbet1 immunoblotting and then confirmed by gel filtration followed by immunoblotting. The velocity gradient-purified rbet1-containing t-SNARE complex was found in gel filtration fractions 16, 17, and 18 (Figure 14, step 2, upper right panel). As was established in previous studies, these fractions contain predominantly rbet1-syntaxin 5-membrin ternary complexes, as well as some rbet1-membrin and rbet1-syntaxin 5 binary complexes. [29]. As a control, soluble rbet1 alone was also subjected to velocity sedimentation, and fractions containing the monomeric rbet1 were pooled and adjusted to a comparable rbet1 concentration as in the SNARE complex fraction. Gel filtration of this fraction confirmed its monomeric state (Figure 14, step 2, upper left panel). Next, the velocity gradient-purified ternary SNARE complex and monomeric rbet1 were separately incubated with p115 prior to gel filtration chromatography. As expected, an rbet1-p115 complex was detected in fractions 10-14 (Figure 14, step 2, middle left panel) when p115 was incubated with monomeric rbet1. However, there was little detectable binding between p115 and the t-SNARE complexes containing rbet1 of similar concentration (Figure 14, step 2, middle right panel). This is the first

direct demonstration that p115 binds stably to a monomeric SNARE but not to the same SNARE when integrated into a SNARE bundle.

Although we cannot exclude that there was a small amount of binding between p115 and the rbet1-syntaxin 5-membrin complex, two experimental factors argue that any such binding was orders of magnitude lower than binding to rbet1 monomers. First, there was some monomer present in the purified complex preparation (Figure 14, step 2, upper right panel, fraction 32). This could account for a slight binding of that preparation to p115 based on a p115-rbet1 binary interaction. Second, the ternary complex preparation is composed primarily of the more binding-active form of rbet1, which is the more rapidly migrating form on SDS-PAGE. Although the structural basis of the two closely-migrating forms is unclear, they are observed in both E.coli-produced as well as endogenous cell extracts [136], with the faster-migrating form exhibiting greater SNARE binding and recruitment to COPII vesicles. The relative efficiency of binding to p115 of the monomer preparation is vastly greater than that of the ternary preparation when only the lower rbet1 band is considered.

D. Membrin Displaces P115 from a Pre-formed Rbet1-P115 Complex

Because p115 is not part of the final SNARE complex, we hypothesized that in order for the SNARE assembly to complete, p115 would need to dissociate from its bound SNAREs. To confirm this prediction, GST-rbet1 or control GST were immobilized on Glutathione-Sepharose beads, then incubated with p115 to allow the formation of a GST-rbet1-p115 complex (Figure 9). After several rounds of

washing to rinse off unbound p115, the beads were incubated either with an excess amount of soluble membrin, or with bovine serum albumin (BSA) as a control. After this incubation, supernatants were collected and the amount of dissociated p115 found in the supernatant was analyzed by immunoblotting. P115 was eluted from the GST-rbet1-p115 beads by membrin in a dose-dependent manner; furthermore, this elution effect pertained to p115 specifically bound to GST-rbet1 beads and not to GST beads (Figure 15A top vs. bottom panels, and quantitated in B). On the other hand BSA had only a small, presumably nonspecific effect on the rbet1-p115 complex that appeared to pertain to non-specifically bound p115 present on either GST or GST-rbet1 beads (Figure 15A, left panels, and quantitated in B).

E. Monomeric SNAREs are a Required Binding Site for P115 on COPII Vesicles

P115 is still associated with membrane in the absence of active Rab1 GTPase [100], suggesting an additional binding site for p115 on the COPII vesicle membrane. SNAREs have been shown to play an essential role in the recruitment of p115 to COPII vesicles [52], yet it is unclear which SNARE species are responsible for this recruitment. So far we have demonstrated that p115 selectively binds to monomeric SNAREs but not SNARE complexes using solution-binding assays, and here we test the hypothesis that p115 requires monomeric SNAREs for its retention on in vitro generated COPII vesicles. This assay utilizes the vesicular stomatitis virus glycoprotein (VSV-G) ts045 as a model cargo. Normal rat kidney (NRK) cells were transfected with myc-VSV-G DNA and cultured at 37°C. Following a subsequent incubation at 40°C that allows VSV-G to accumulate in the ER, cells were

permeablized and incubated in the presence of rat liver cytosol, an ATP regenerating system, and buffer, allowing them to produce COPII coated vesicles with a cytoplasmically accessible myc tag. These vesicles were incubated in the presence or absence of recombinant soluble rbet1, then immuno-isolated using anti-myc antibody beads (Figure 16A). The amount of p115 present on the vesicles, as well as internal membrane markers, was analyzed by immunoblotting. Compared to the control, the addition of excess soluble rbet1 removed all detectable p115 from the COPII vesicles (Figure 16B). The fact that a soluble SNARE alone can compete p115 off vesicle membranes suggests that monomeric SNAREs account for the p115 interactions with COPII vesicles—or at least for those ongoing p115 interactions strong enough to withstand the immuno-isolation of vesicles. This finding is consistent with, but more direct than previous studies showing that an inhibition of SNARE complex disassembly impairs p115-membrane association [52, 100].

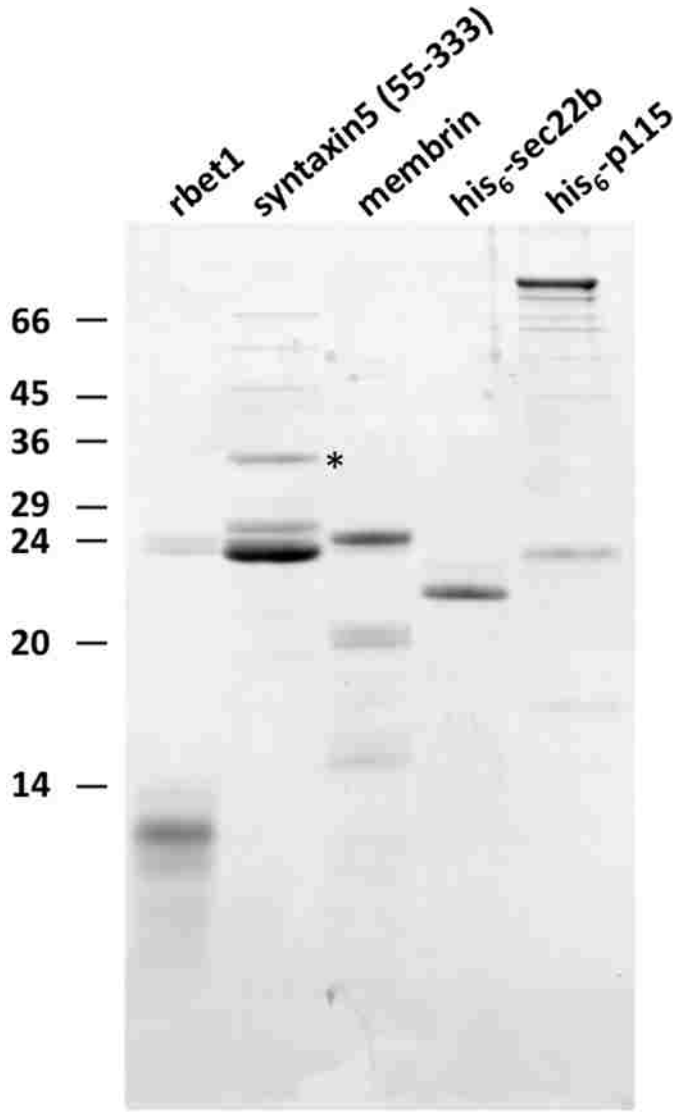

Figure 11. Purified recombinant SNAREs and p115. Proteins were separated on a 15% SDS-PAGE gel, and stained with Coommassie Blue. Protein loads correspond to the relative amounts used in gel filtration binding assays. Rbet1 (residues 1-95) runs below the 14 kD marker and contains sub-stoichiometric GST contaminants around the 24 kD marker. Syntaxin 5 (residues 55-333) runs between the 29 and 36 kD markers (marked by an asterisk) and contains heavy GST contamination around the 24 kD marker. A C-terminal truncation product of syntaxin 5 lacking the SNARE motif (residues 55-251) runs between the 24 and 29 kD markers. Bands above the 45 kD marker represent uncleaved GST fusion proteins and their C-terminal truncation products. The full-length membrin band between 24 and 29 kD markers is largely free of contaminating GST but contains sub-stoichiometric unknown truncation or degradation products. His6-sec22b between the 20 and 24 kD markers is largely homogeneous. His6-p115 runs above the 97 kD marker and contains various unknown C-terminal truncation products and a substantial contaminant near the 24 kD marker (see Fig. 17B for detail).

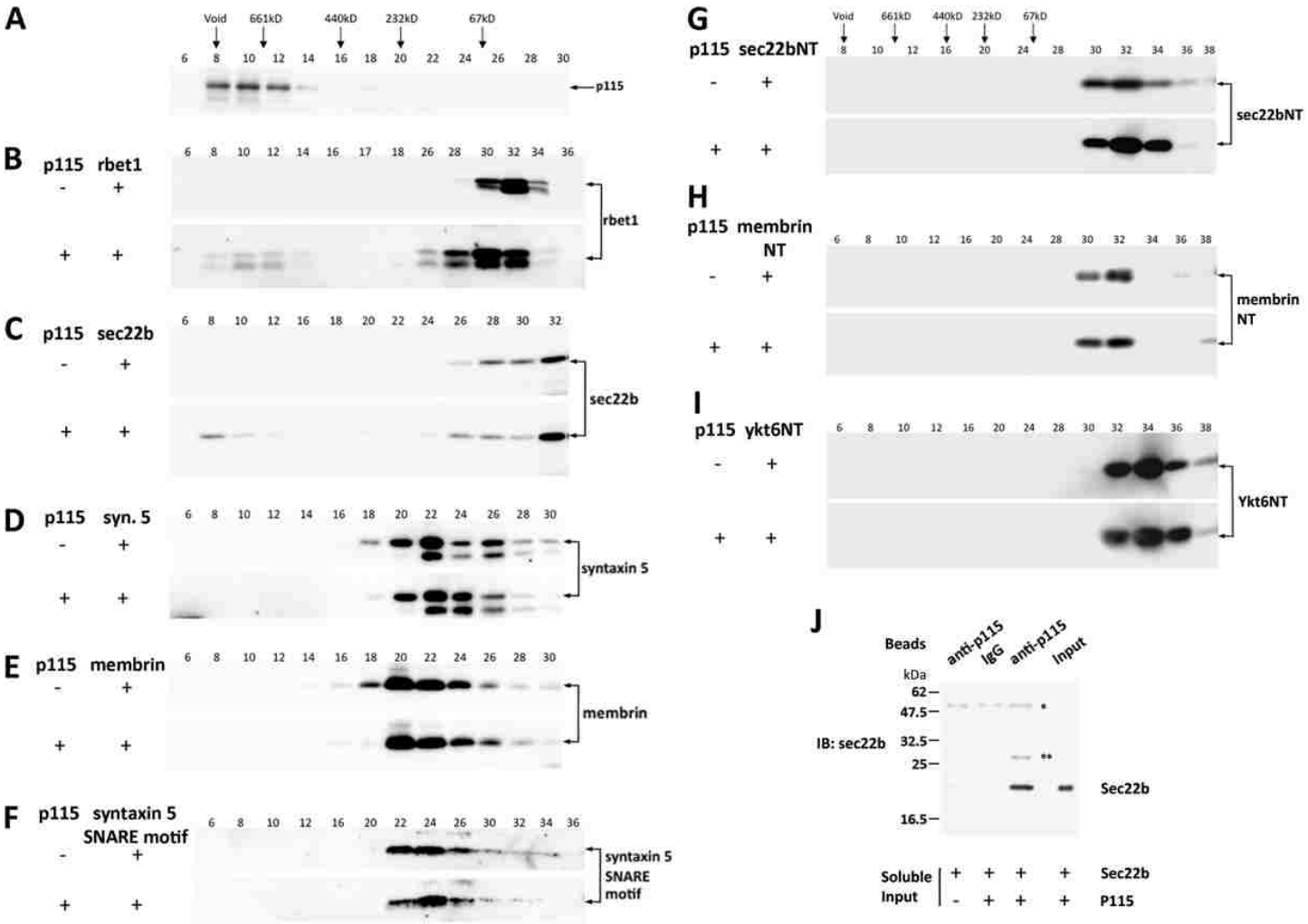
A
Void
661kD
440kD
232kD
67kD
p115
B
p115 rbet1
rbet1
C
p115 sec22b
sec22b
D
p115 syn. 5
syntaxin 5
E
p115 membrin
membrin
F
p115 syntaxin 5 SNARE motif
syntaxin 5 SNARE motif
G
p115 sec22bNT
sec22bNT
H
p115 membrin NT
membrin NT
I
p115 ykt6NT
Ykt6NT
J
Beads
anti-p115
IgG
anti-p115
Input
kDa
62
47.5
32.5
25
16.5
IB: sec22b
Sec22b
Soluble
Input
Sec22b
P115

Figure 12. Binary interactions of p115 with ER-Golgi SNAREs rbet1 and sec22b, but not syntaxin 5, membrin, or SNARE N-terminal domains. Soluble recombinant p115, syntaxin 5, membrin, rbet1, and sec22b were passed through a Superdex 200 column separately, fractions were collected and analyzed by Western blotting. The SNAREs were then each incubated separately with 1.3 μM p115 overnight on ice, the reactions were gel-filtered and analyzed by Western using anti-SNARE antibody. (A) P115 only elution. (B) Rbet1 only (top) and rbet1-p115 reaction mix (bottom) elutions. (C) Sec22b only (top) and sec22b-p115 reaction mix (bottom) elutions. (D) Syntaxin 5 only (top) and syntaxin 5-p115 reaction mix (bottom) elutions. (E) Membrin only (top) and membrin-p115 reaction mix (bottom) elutions. (F) Syntaxin 5 (residues 55-333) was subjected to thrombin cleavage. The SNARE motif (residues 251-333) was purified by velocity sedimentation on 5–30% glycerol gradients. Top panel: Syntaxin 5 SNARE motif only elution. Bottom panel: Elution of syntaxin 5 SNARE motif-p115 reaction mix. Hexahistidine-tagged N-terminal domain constructs of sec22b, membrin, and Ykt6 were expressed in E. coli and purified by nickel-affinity chromatography (see Materials and Methods). Sec22b NT (G), membrin NT (H), and Ykt6 NT (I) were passed through gel filtration column separately (top panels). Each protein was then incubated with p115 and then the mixed reactions were gel-filtered and immunoblotted with anti-SNARE antibodies (bottom panels). Gel filtration fraction numbers are shown above top panels. Elution positions of Dextran 2000 (void), native thyroglobulin (669 kDa), ferritin (440 kDa), catalase (232 kDa), and BSA (67 kDa) are indicated with arrows above the fraction numbers. (J) sec22b and p115 were co-incubated as in part C, centrifuged at 100,000 x g to remove potential aggregates, and then precipitated using α-p115 antibody beads. The presence of specifically co-precipitated sec22b demonstrates the presence of a soluble p115-sec22b complex. "*" marks IgG heavy chain; "**" marks a contaminant in the p115 preparation that cross-reacts with the anti-sec22b antibody.

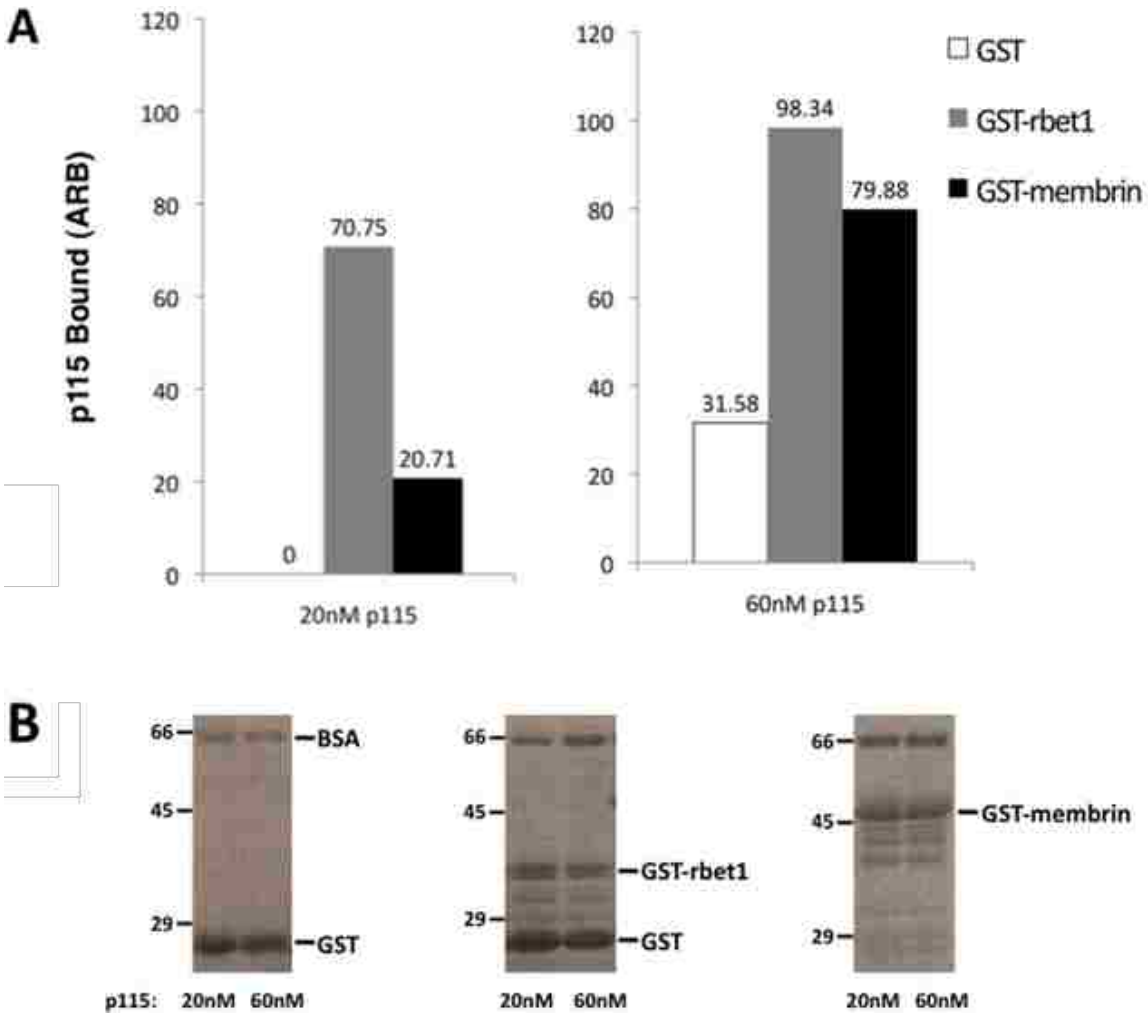

Figure 13. P115 binds to bead-immobilized GST-rbet1 with higher affinity than GST-membrin. (A) Binary bead-binding experiments were carried out as described in MethodsP115 binding to GST, GST-rbet1, and GST-membrin beads, at the two assayed concentrations. (B) Ponceau S staining of membrane demonstrate that similar amounts of bead-immobilized fusion proteins were present in each reaction.

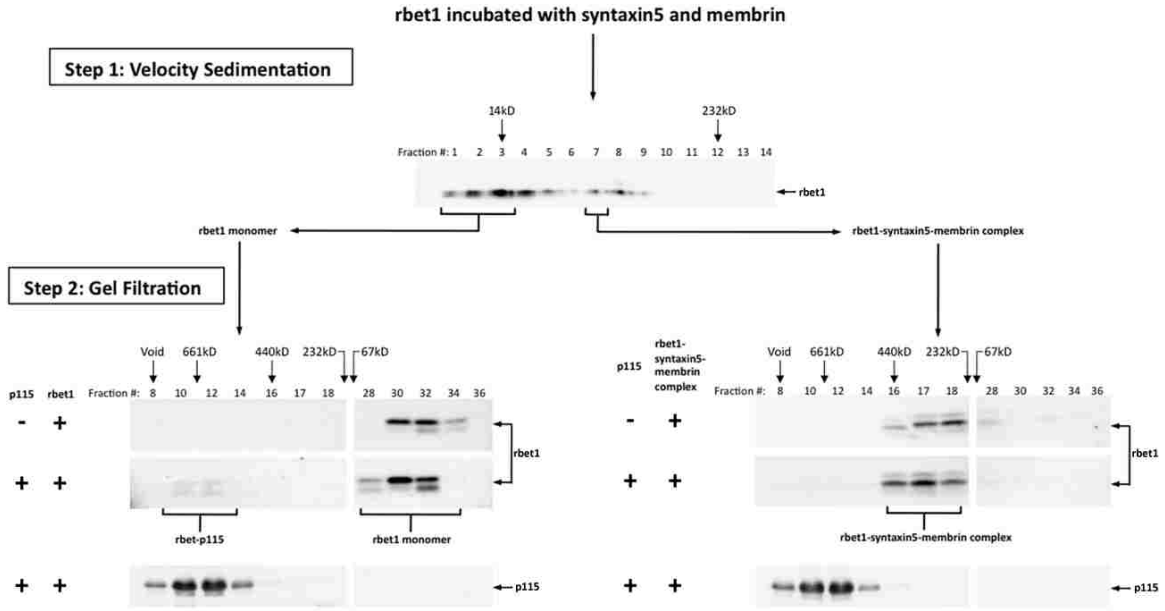

Figure 14. P115 binds monomeric rbet1, but not t-SNARE complexes containing rbet1. Recombinant rbet1 was incubated with recombinant syntaxin 5 and membrin overnight on ice to allow the formation of SNARE complexes. Reaction mix was loaded onto a 5–30% glycerol gradient, and subjected to velocity sedimentation (Step 1). The presence of t-SNARE complexes in fraction 7 was confirmed by Western blotting (data not shown). Recombinant rbet1 alone was also subjected to velocity sedimentation, and fractions containing monomeric rbet1 were pooled and adjusted to a similar rbet1 concentration as the SNARE complex (for simplicity this is depicted as a pool of those fractions from the complexes gradient). Both monomeric rbet1 and SNARE complex were passed through a gel filtration column, with fractions analyzed by Western blotting using an anti-rbet1 antibody (Step 2, top panels). Monomeric rbet1 and the SNARE complex were incubated with p115 separately, the mixed reactions were gel-filtered and analyzed by Western blotting using the same antibody (Step 2, middle panels). P115 in the mixed reaction fractionation was also detected by immunoblot (Step 2, bottom panels).

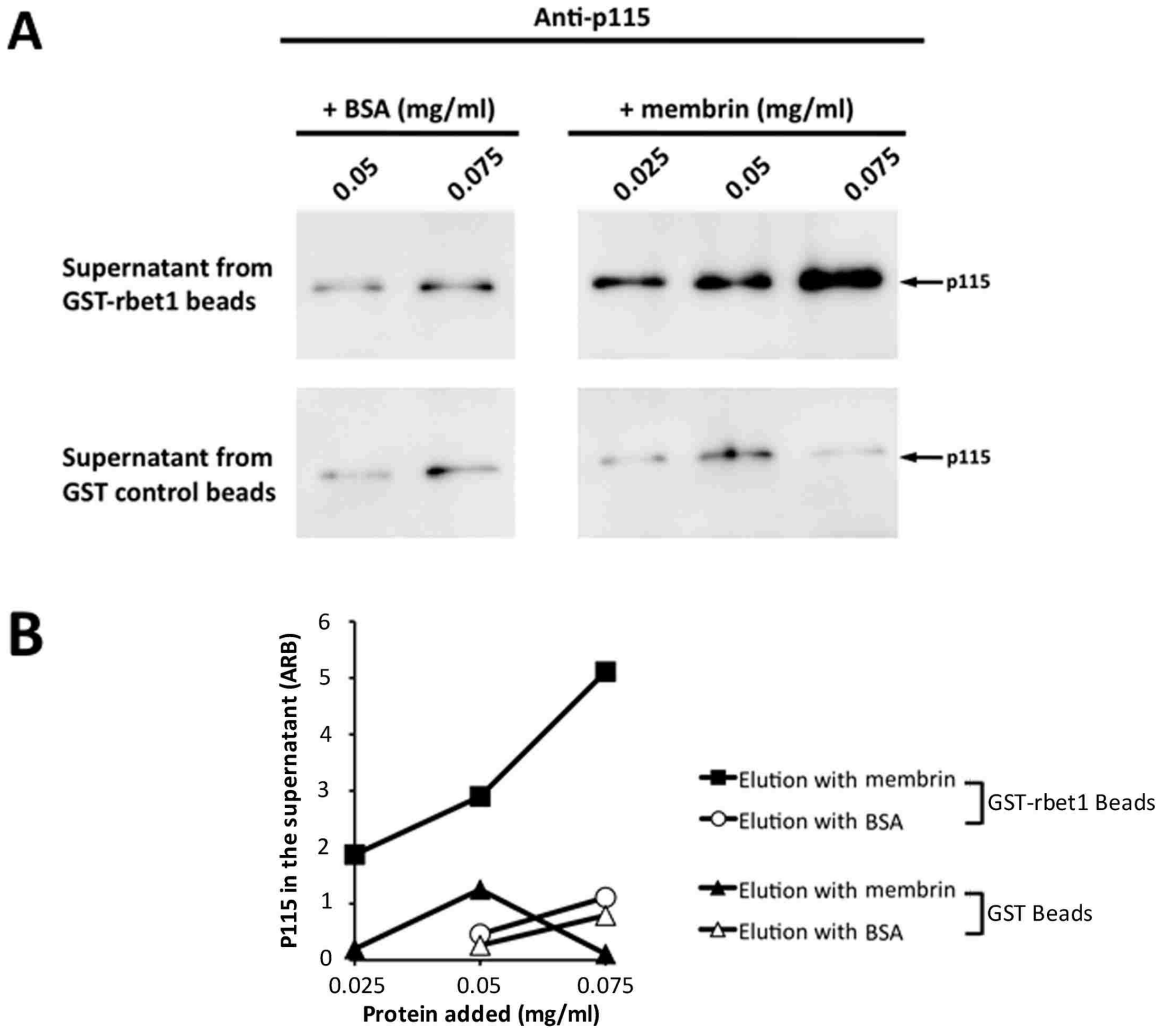

Figure 15. Soluble membrin displaces p115 from a pre-formed p115-rbet1 complex. Displacement experiments were carried out as described in Methods. In short, GST or GST-rbet1 was immobilized on glutathione-Sepharose beads. Beads containing 0.5 mg/ml GST-rbet1 or GST were then incubated with 600 nM p115 at 4°C overnight to allow the formation of p115-rbet1 complexes. After thorough washing, increasing concentrations of membrin or control BSA were added to the p115-treated beads. Following an incubation of 1 hr at 4°C, beads were centrifuged, supernatants were harvested, and p115 present was analyzed by SDS-PAGE and Western blotting. (A) Amounts of p115 present in the supernatants from GST beads (bottom panels) or GST-rbet1 beads (top panels) incubated with BSA or membrin as indicated. (B) Quantitation of blots from panel B.

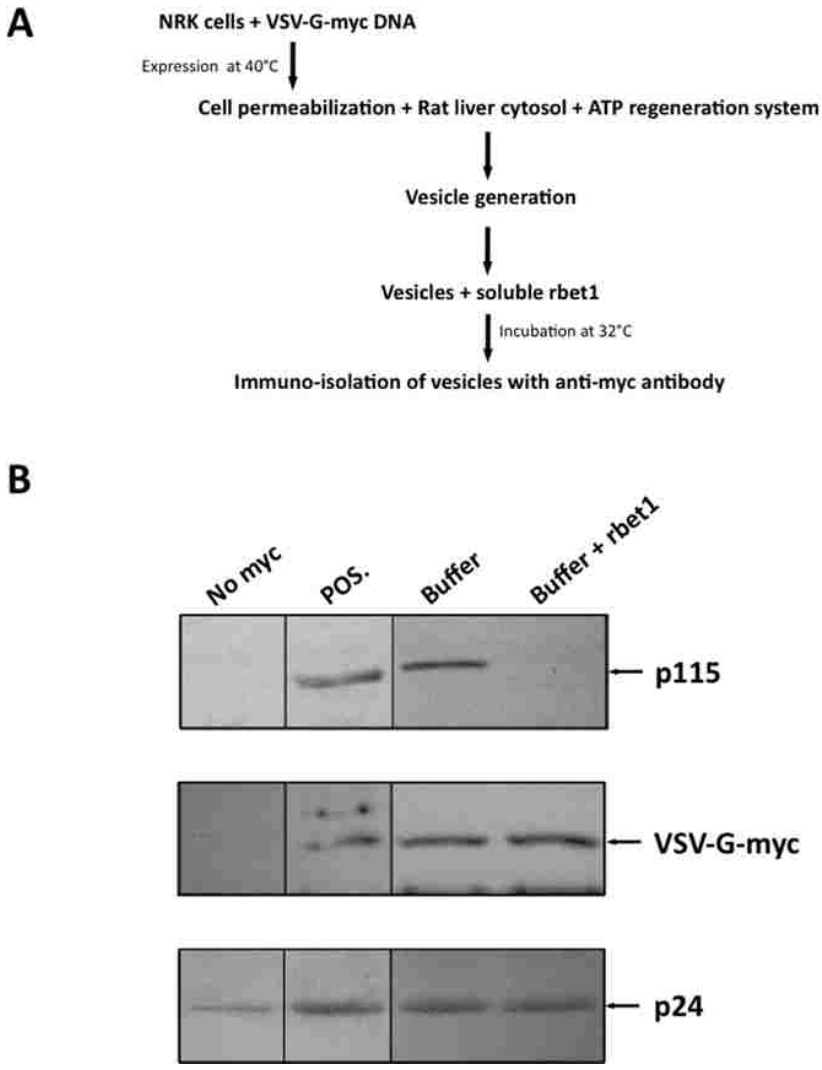

Figure 16. Excess soluble rbet1 removes p115 from COPII vesicle membranes. (A) Normal rat kidney (NRK) cells were transfected with myc-VSV-G DNA, infected with vaccinia virus to drive over-expression (see Methods), and incubated at 40°C to allow the accumulation of myc-VSV-G in the ER. The cells were then permeabilized at 40°C and incubated with rat liver cytosol in the presence of an ATP regeneration system. Generated COPII vesicles were separated from cells by centrifugation. 0.3 μM of soluble rbet1 was added to the vesicles followed by an incubation of 1 hr. Vesicles were then immunoisolated using the myc tag. The recombinant rbet1 used in this experiment was dialyzed extensively in Buffer A. To eliminate any potential effects caused by the buffer, similar amount of Buffer A was also added to the vesicles as control. (B) Isolated vesicles were subjected to SDS-PAGE and amounts of p115 (top panel), cargo myc-VSV-G (middle panel), and vesicle membrane marker p24 (bottom panel) were determined by immunoblotting. Vesicles generated by untransfected NRK cells served as negative control; vesicles generated by myc-VSV-G transfected cells without rbet1 or Buffer A addition served as positive control.

Chapter IV. P115's Role in SNARE Complex Assembly

The formation of a Sed5p/Sec22p/Betlp SNARE complex in yeast requires the presence of the yeast p115 homologue Uso1p [96]. Also, p115 stimulates the assembly of GOS-28–syntaxin-5 SNAREpin in vitro [116]. Since p115 bound to monomeric SNAREs in our studies, we wondered whether this binding had a detectable effect on SNARE complex assembly.

Soluble recombinant syntaxin 5, membrin, rbet1 and sec22b were incubated on ice either in the presence or absence of p115 for four hours. Reaction mixtures were gel-filtered, and the fractions analyzed by immunoblotting. Quaternary SNARE complexes are eluted from the gel filtration column in fractions 16, 17, 18 [29]. To distinguish between the complete quaternary complex and ternary or binary SNARE complexes whose elutions overlapped the same fractions, an antibody against the v-SNARE sec22b was used, for sec22b only enters into a SNARE complex when all three of its cognate binding partners are present in a single complex [29]. As is typical, only a small fraction of sec22b was incorporated into quaternary complexes. Unexpectedly, we were not able to detect a stimulatory effect of p115 on the SNARE assembly, though p115-sec22b complexes were clearly present in fractions 8-10 (Figure 17A).

One possibility that could explain the lack of stimulatory effects was that p115 binding has a stabilizing effect on SNARE conformation rather than an immediate catalytic effect. We therefore tried a different approach. Sec22b was pre-incubated overnight with or without p115, before the addition of other SNAREs.

After a second incubation of four hours to allow the formation of SNARE complexes, both reactions were passed through a gel filtration column and SNARE complexes were quantified and compared. As shown in Figure 17B, the long pre-incubation of sec22b with p115 enhanced the formation of SNARE complex by at least two-fold. Adding rbet1 to the pre-incubation mixture of sec22b and p115 did not cause any additional enhancement of the complex formation (data not shown). Our findings suggest that p115 may have a mild 'chaperone' effect on the SNAREs, possibly by binding to the SNARE motif and keeping it in an optimal conformation for complex assembly. This prediction does not necessarily contradict the catalyst model, for p115 could still function as a SNARE catalyst downstream. Three caveats of this purified experimental system that could also explain the lack of apparent catalytic activity are the lack of cofactors required for p115's function, the lack of membrane topological constraints, and the possibility that purified recombinant p115 was not fully functional.

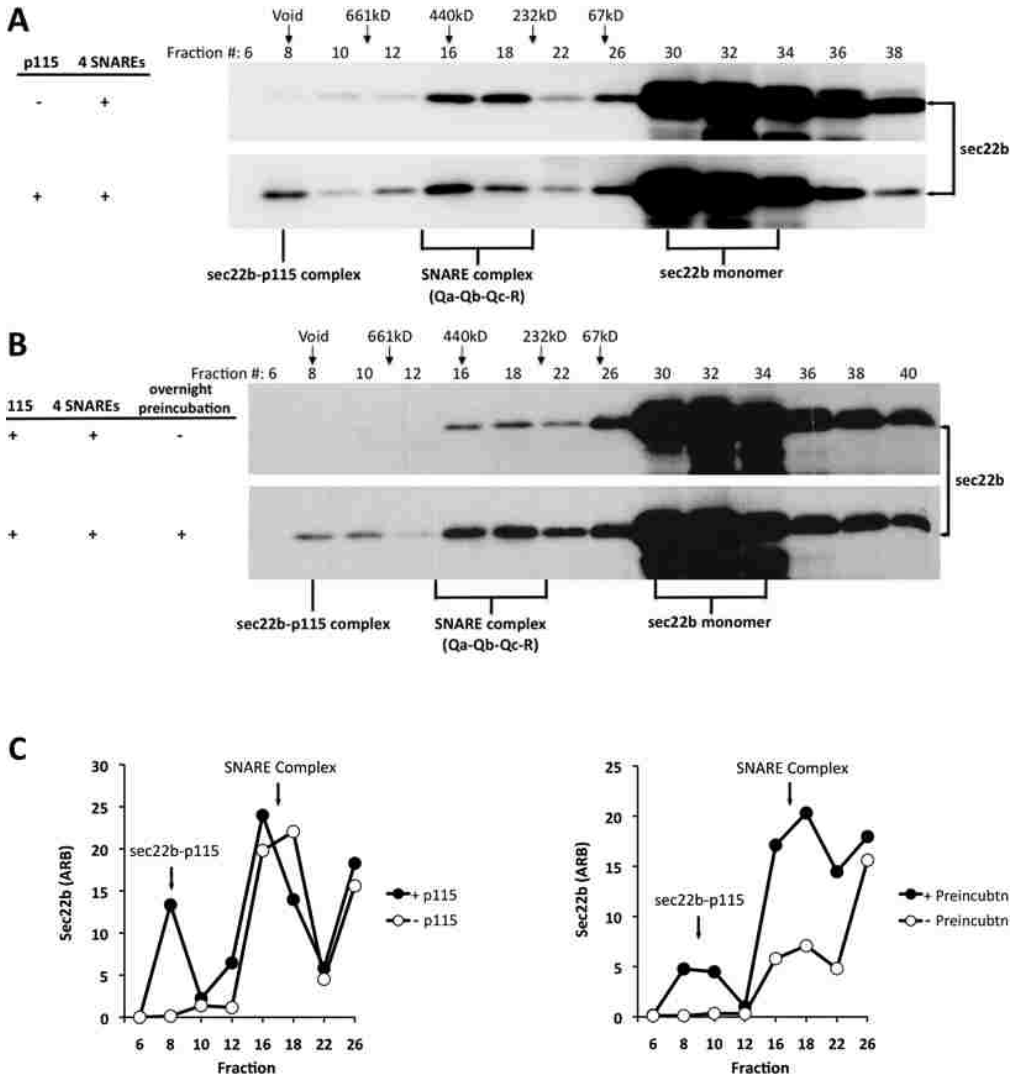

Figure 17. P115 chaperone effect on SNARE complex assembly. (A) Recombinant syntaxin 5, membrin, rbet1, and sec22b were incubated in the presence or absence of 0.9 μM His6-p115 for 4 hrs on ice. The reactions were passed through a gel filtration column. Fractions were analyzed with SDS-PAGE and immunoblotting using anti-sec22b antibody. The sec22b-syntaxin 5-membrin-rbet1 complex elutes in fractions 16-18. (B) P115 was incubated with sec22b overnight on ice. The next day, other SNAREs were added to the reaction mixes and incubated for 4 hrs on ice. Reactions were then gel-filtered and analyzed as described in (A). Top panel in (B) represents the elution of a SNARE assembly reaction carried out in the presence of a similar concentration of p115 but without any overnight pre-incubation between p115 and sec22b. The absence of a p115-sec22b binary complex in the top panel of (B) was likely due to relative short incubation time (4 hrs as opposed to overnight, as in the bottom panel). (C) Quantitation of A (left panel) and B (right panel) fractions 6 through 26. Beyond fraction 26, the chemiluminescence signal saturated the camera pixels and quantitative data was not possible.

Chapter V. Excess Recombinant P115 Inhibits P115 Function *in vitro* and *in vivo.*

A. P115's Effects on COPII Vesicle Tethering and Fusion *in vitro*

A requirement for p115 in COPII vesicle transport has been demonstrated before [50, 99, 137], but the precise steps at which p115 is involved in the tethering and fusion of COPII vesicles has not been resolved. We have developed in vitro assays of COPII vesicle tethering and fusion in which two distinctly labeled, fusogenic COPII vesicle populations are generated from permeabilized normal rat kidney (NRK) cells, one carrying the myc tag, the other radiolabeled by ^{35}S [3, 52]. Notably, if the two vesicle populations are co-incubated at 32°C, fusion of the differently labeled vesicles results in a heterotrimer containing both a myc-labeled VSV-G subunit and a ^{35}S labeled VSV-G* subunit, due to the dynamic equilibrium between VSV-G trimers and monomers [126]. To detect fusion, the mixtures are detergent-solubilized and VSV trimers are immunoprecipitated using the myc tag. In this protocol, fusion is a function of the ^{35}S labeled VSV-G trimers present in the solubilized vesicles. To detect tethering, the two populations of COPII vesicles are incubated together at 32°C and immuno-isolated intact without solubilization using anti-myc antibody beads. The beads are then analyzed by SDS-PAGE and autoradiography for the presence of ^{35}S-VSV-G, which represents co-isolated, physically associated vesicles.

To test p115's effects on vesicle fusion, we first generated a p115-free cytosol to use in the assay. Rat liver cytosol was incubated with a p115 antibody before depletion with fixed S. aureus cells. The depletion of p115 was complete as shown in

Figure 18A, top left panel. Amounts of several known p115-interacting partners were also analyzed by Western. With the exception of GM130, none were affected. GM130 is a primarily Golgi-localized tether and was implicated to function at a later step in ER-Golgi anterograde transport independently of p115 [138]. There has been no evidence suggesting GM130 may affect homotypic COPII vesicle fusion. Thus we did not expect a partial co-depletion of GM130 to have a significant effect on the COPII vesicle tethering/fusion assay. A 'mock' cytosol treated with non-immune rabbit IgG was used as control.

To test the functional effects of p115 depletion and the back-addition of recombinant p115, myc-VSV-G vesicles and 35^S-VSV-G vesicles were mixed and incubated in either p115-free cytosol or mock-treated cytosol, with or without additional purified recombinant p115, and fusion was monitored. Fusion levels were normalized to the level in untreated RLC. Depletion of p115 reduced vesicle fusion by 70% of mock (Figure 18C, red versus blue curves at zero point on x-axis). This extends previous antibody inhibition studies [52] implying that p115 is required at the first fusion step in the secretory pathway, leading to VTC biogenesis. Recombinant p115 failed to restore fusion activity, although we observed a small stimulation at a concentration of 0.1 μM (Figure 18C, red curve). The reasons for the lack of rescue are not clear. It is possible that the optimal dose range for p115's function is very narrow (see Discussion), and we were not able to pinpoint the concentration at which sufficient p115 is provided yet the ratio and/or access of p115 to its cofactors (e.g. Rab1) is close to physiological. Surprisingly, though, recombinant p115 seemed to have a strong inhibitory effect on vesicle fusion when

added in excess to the endogenous protein in mock-depleted cytosol (Figure 18C, blue curve). The p115 preparation employed in these studies was the Ni-NTA fraction shown in Figure 18B.

We wanted to understand the unexpected inhibitory effect of wild type recombinant p115. To eliminate the possibility that a truncated, dominant-negative form of p115 was present in the protein preparation, we further purified the Ni-NTA enriched p115 with Mono Q anion exchange chromatography (Figure 18B, also see Materials and Methods). Although many partial products were removed by the additional step, the purified fraction still contained a low molecular weight degradation/truncation fragment of p115. Since we were unable to prepare the full-length protein without this contaminant, we purified the small fragment to near-homogeneity by velocity sedimentation (Figure 18B, third lane) and used it as a control in subsequent experiments. When titrated in the presence of untreated cytosol, the Mono Q-purified full-length p115 inhibits both fusion (Figure 18D) and tethering (Figure 18E) of COPII vesicles in a dose dependent manner. Neither buffer control nor the p115 small fragment had any effects on fusion or tethering activities. Thus, inhibitory activity appears to reside with the full-length protein. We observed a small stimulation of vesicle tethering by recombinant p115 in low excesses (0.002 μM, Figure 18E). This effect was not present in the fusion experiment (Figure 18D). On the other hand, we noted that compared to the tethering assay, the fusion assay required lower concentrations of excess p115 to reach the maximum inhibitory effect. It is possible that the fusion of vesicles is more sensitive to changes in p115 concentration than vesicle tethering. In summary, recombinant full-length p115 had

very slight stimulatory effects at very low concentrations that were overcome by potent inhibitory activity in both the presence and absence of endogenous p115.

B. Excess P115's Effects on the Secretory Pathway *in vivo*

To test whether excess p115 also inhibited p115 trafficking function in vivo, we over-expressed full-length, functional p115 in HeLa cells. As shown in Figure 19A-C, overexpression of a myc-tagged p115 construct in vivo causes disruption of HeLa cell Golgi structure monitored with GM130 labeling. Golgi disruption clearly correlated with p115 expression level, since moderately expressing cells displayed morphologically normal Golgis. We know that the myc-tagged construct was intrinsically functional, since when expressed at moderate levels it restored the normal GM130 pattern to p115-depleted cells with otherwise dispersed Golgis (Figure 19D-F). Phenotypes of siRNA depletion of p115 in HeLa cells have been characterized earlier [114].

It would appear that p115 has a tight functional dose range. A certain level of p115 is required for COPII vesicle tethering and fusion, yet these events are inhibited when the tether is present in excess. These findings are in line with our SNARE-binding results, which suggest that p115 needs to be removed from SNARE complexes prior to their completion. One would expect that excess p115 might inhibit SNARE-mediated fusion by slowing down or preventing this removal process.

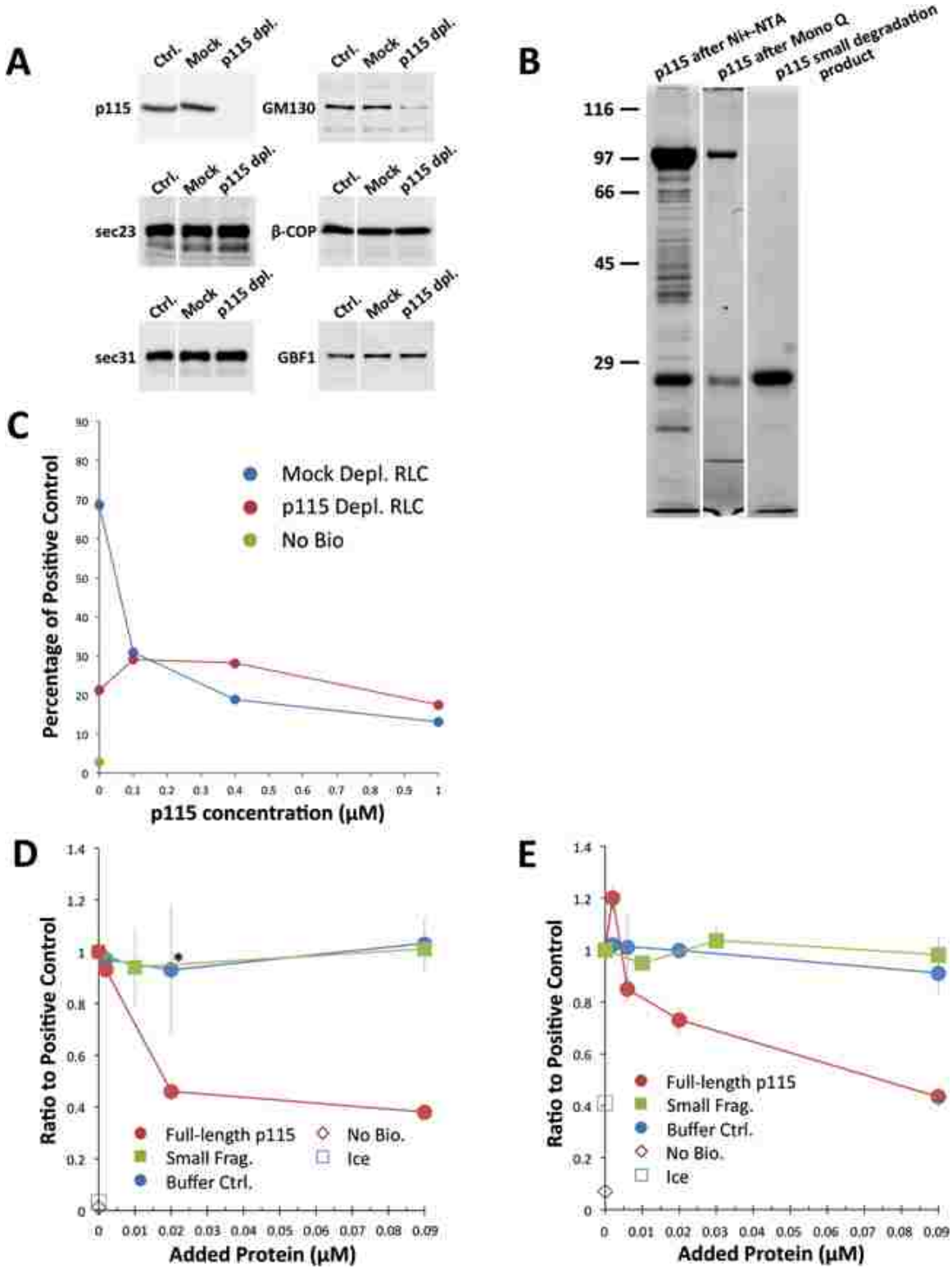
A
Ctrl.
Mock
p115 dpl.
p115
GM130
sec23
β-COP
sec31
GBF1
B
p115 after Ni+-NTA
p115 after Mono Q
p115 small degradation product
116
97
66
45
29
C
Percentage of Positive Control
Mock Depl. RLC
p115 Depl. RLC
No Bio
p115 concentration (μM)
D
Ratio to Positive Control
Full-length p115
Small Frag.
Buffer Ctrl.
No Bio.
Ice
Added Protein (μM)
E
Ratio to Positive Control
Full-length p115
Small Frag.
Buffer Ctrl.
No Bio.
Ice
Added Protein (μM)

Figure 18. Recombinant full-length p115 inhibits in vitro COPII vesicle tethering and fusion. (A) Depletion of p115 from rat liver cytosol. Rat liver cytosol was treated with rabbit anti-p115 antibody (p115 dpl.), or purified rabbit IgG (Mock) for 2 hrs on ice, and depleted with fixed S. aureus cells for 15 min. (Ctrl.) represents RLC without any treatment. Amounts of p115, GM130, sec23, beta-COP, sec31, and GBF1 were analyzed after depletion. (B) Ni-NTA purified recombinant His6-tagged p115 (left lane) was further purified on a Mono Q column (middle lane). The small truncation fragment of p115 was purified from the full-length protein preparation by velocity sedimentation (right lane). (C) Both p115 depletion and recombinant p115 addition inhibits in vitro COPII vesicle fusion. Myc-tagged and ^{35}S-tagged VSV-G COPII vesicles were incubated together at 32^{o}C for 1 hr, either in the presence of mock-depleted cytosol (blue curve) or p115-depleted cytosol (red curve), and the indicated concentrations of recombinant p115 ranging from 0.1-1 μM (x-axis) was added to the reactions. After adding Triton X-100, VSV-G trimers were immunoprecipitated using the myc tag and heterotrimers containing ^{35}S were quantitated as a measure of fusion. Fusion was normalized to percentage of the positive control reaction in which untreated RLC was used and no additional protein was added. Ice control (green) indicates fusion reactions incubated on ice. Data points at zero p115 concentration are representative of triplicate reactions, with error bars representing S. D. The remaining data points were obtained from singlicate reactions. The experiment was repeated three times with qualitatively similar outcomes. (D) COPII vesicle fusion in the presence or absence of recombinant Mono Q purified p115. Myc-tagged and ^{35}S-tagged VSV-G COPII vesicles were incubated together at 32°C for 1 hr in the presence of untreated RLC with normal level of endogenous p115 and the indicated concentrations of Mono Q p115 (red curve) or p115 small fragment (green curve) ranging from 0.002-0.09 μM. Triton X-100 was added to the reactions and VSV-G heterotrimers were immunoprecipitated and quantitated as described above. Due to the high KCl content of the Mono Q column elution buffer, we also tested Mono Q elution buffer (blue curve). Fusion was normalized to percentage of the buffer control with no additional p115. The no-bio control represents signal obtained from pellets isolated with non-biotinylated myc antibody. Data points are duplicates, with error bars representing S.E.M. The asterisk marks a control data point that resulted in p=.027 in a two-tailed T-test with the corresponding full-length p115 data point. (E) COPII vesicle tethering in the presence or absence of recombinant p115. Myc-tagged and ^{35}S-tagged VSV-G COPII vesicles were incubated together at 32°C for 1 hr with untreated RLC and the indicated concentrations of Mono Q purified p115 (red curve), p115 small fragment (green curve), or Mono Q buffer control (blue curve). Intact vesicles were immunoisolated in the absence of detergent using the myc tag and recovered ^{35}S-VSV-G quantitated as a measure of tethering. Tethering was normalized to percentage of the buffer control with no additional p115. Data points at 0.002 μM protein concentration were obtained from quadruplicate reactions, other data points are representative of duplicates. Error bars represent S.E.M. The experiments in D and E were repeated twice with similar outcomes.

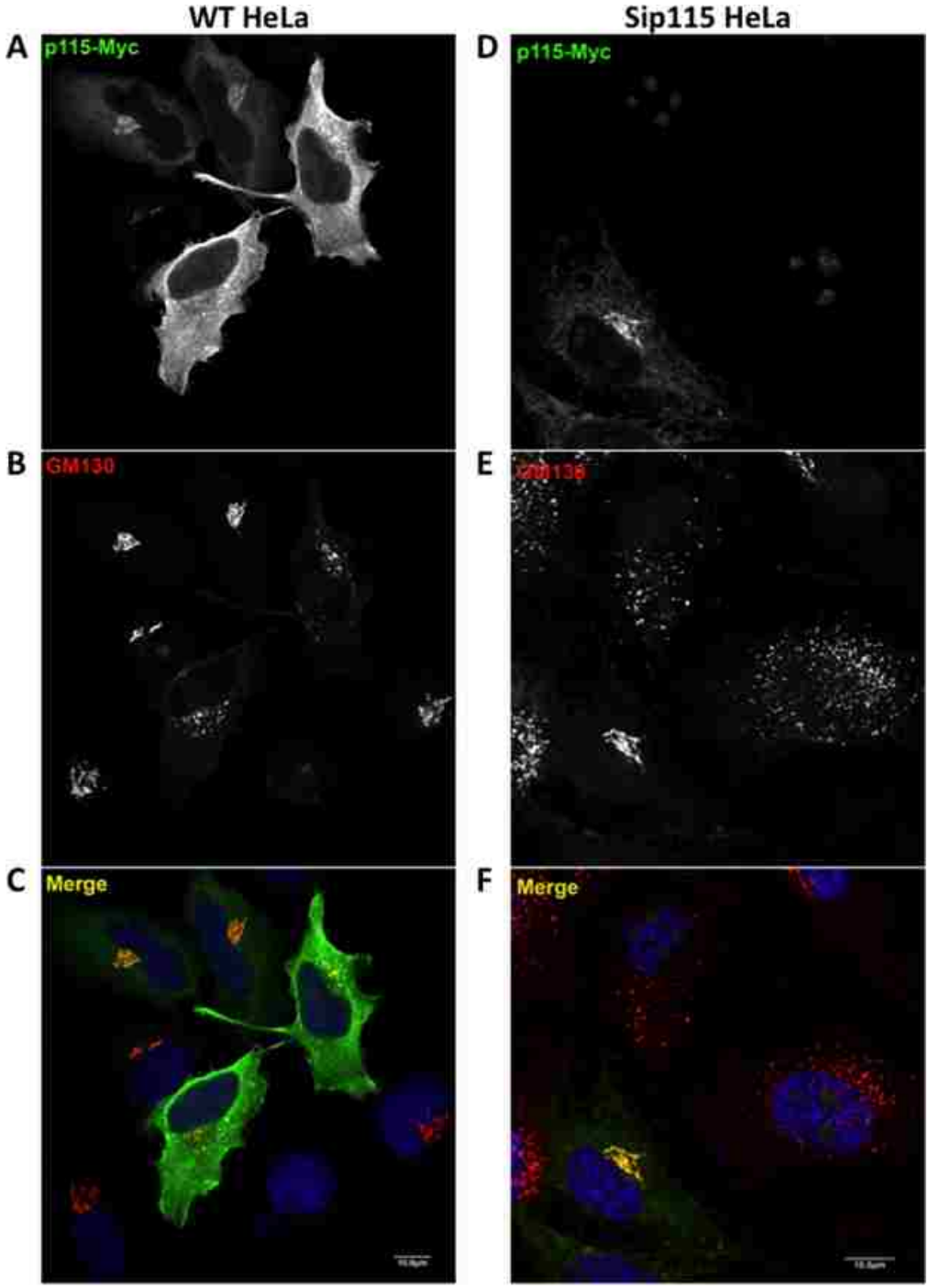

Figure 19. Effects of full-length myc-tagged p115 in vivo. HeLa cells overexpressing myc-p115 labeled with anti-myc antibodies (A) displayed disrupted Golgi morphology, as indicated by labeling of the Golgi marker GM130 (B). The same myc-p115 construct, when expressed at moderate levels in p115-knockdown cells (D), rescued the Golgi fragmentation phenotype caused by p115 depletion, as indicated by GM130 labeling (E). This experiment was performed by Robert Grabski at the University of Alabama, Birmingham.

Chapter VI. Binding Properties of a Functional, Endogenous Rat Liver P115 Recapitulate Purified Recombinant P115

We wanted to validate the most important conclusions from purified SNARE binding studies in Figures 12-16 using functionally robust, endogenous p115. A partially purified liver p115 could potentially provide optimal functional intactness and yet also likely reflect the intrinsic binding properties of p115. Toward this end, we prepared rat p115 at three increasing levels of enrichment. First was crude NRK cytosol from cells expressing rat his-p115 (referred to as "NRK cytosol"; immunnoblot analysis not shown). Second was endogenous rat liver p115 purified by ammonium sulfate fractionation and Superdex 200 chromatography (referred to as "rat liver Superdex"), enriched approximately 18-fold relative to crude rat liver cytosol. This fraction is characterized by immunoblotting in Figure 20D. Third was endogenous rat liver p115 purified by several conventional chromatography steps to yield a simplified protein pattern with p115 representing a major band (referred to as "rat liver Mono Q"). This fraction is characterized by Coommassie gel in Figure 20B, left panel. Next we evaluated whether rat p115 at different purity levels would behave similarly in SNARE bead binding assays. As shown in Figure 20A and B, when tested at a limiting concentration, "NRK cytosol" p115 and "rat liver Mono Q" p115 bound specifically to SNARE beads with similar characteristics--weak binding to membrin and strong binding to rbet1, as observed in Figure 13 with purified recombinant His-p115 expressed in bacteria. SNAREs immobilized on the beads are characterized by Coommassie gel in Figure 20B, right panel.

Given the apparent robustness of the SNARE bead binding assay with regard to

p115 purity, we chose to confirm and extend our main conclusion, that p115 prefers to bind SNARE monomers and not complexes, using the endogenous rat liver Superdex fraction, since it represented a compromise between biochemical purity and likely functional intactness. Importantly, when tested in an ER-to-Golgi transport reconstitution in semi-intact NRK cells [127], the Superdex p115 fully reconstituted transport activity to p115-depleted cytosol, indicating that it was functionally intact (Figure 20C, solid circles). This was important since we found that further purified p115 preparations from various sources only partially restored activity and/or lost activity readily (not shown), perhaps due to the lack of cofactors or stabilizing interactions. The p115 in the Superdex fraction was required for the reconstituting activity, as opposed to other rate-limiting factors, since p115 antibody depletion blocked the reconstitution (Figure 20C, open circles).

To test whether the rat liver p115 bound to SNAREs but not SNARE complexes, we prepared GST-rbet1 beads, GST-membrin beads, and beads that contained a stoichiometric complex of GST-membrin and rbet1 (Figure 20E. The Superdex p115 fraction was incubated with each of the beads and unbound or loosely bound proteins were removed by washing. As shown in Figure 20F, the p115 bound most strongly to the rbet1 beads, but at the concentration tested also significantly interacted with membrin beads. Strikingly, no specific binding was detected to the membrin•rbet1 beads, despite the presence of stoichiometric amounts of two proteins it interacted with separately. The rbet1 preparation on these beads was identical to the soluble rbet1 used for Figures 12 and 14, which bound p115 very well. Additionally, the membrin and rbet1 employed in the binary

complex were fully capable of forming higher order complexes, since together they exhibited potentiated binding with soluble syntaxin 5, indicating formation of a ternary SNARE complex (Figure 20G) [29]. In conclusion, functionally intact endogenous rat liver p115 bound to individual SNAREs but not SNARE complexes, extending and validating the conclusions from purified recombinant proteins.

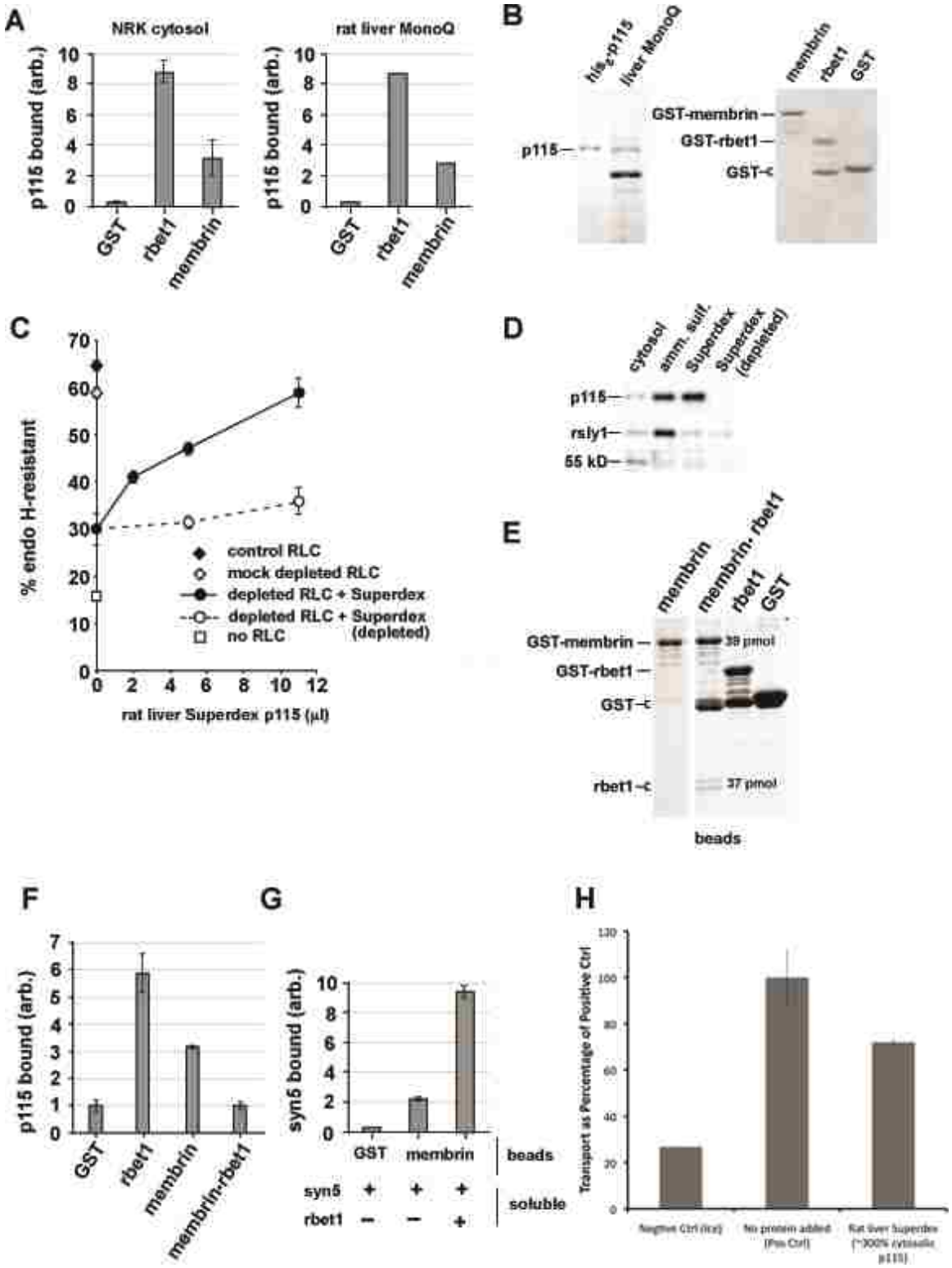
A
NRK cytosol
rat liver MonoQ
p115 bound (arb.)
GST
rbet1
membrin
B
his6-p115
liver MonoQ
membrin
rbet1
GST
p115
GST-membrin
GST-rbet1
GST-c
C
% endo H-resistant
control RLC
mock depleted RLC
depleted RLC + Superdex
depleted RLC + Superdex (depleted)
no RLC
rat liver Superdex p115 (µl)
D
cytosol
amm. sulf.
Superdex
Superdex (depleted)
p115
rsly1
55 kD
E
membrin
membrin- rbet1
rbet1
GST
GST-membrin
GST-rbet1
GST-c
39 pmol
rbet1-c
37 pmol
beads
F
p115 bound (arb.)
GST
rbet1
membrin
membrin-rbet1
G
syn5 bound (arb.)
GST
membrin
beads
syn5
rbet1
soluble
H
Transport as Percentage of Positive Ctrl
Negative Ctrl (Ica)
No protein added (Pos Ctrl)
Rat liver Superdex (~300% cytosolic p115)

Figure 20. Binding properties of endogenous rat liver p115. (A) GST, GST-rbet1, or GST-membrin were immobilized on glutathione-Sepharose beads. Beads were incubated with crude or partially purified fractions, "NRK cytosol" and "rat liver MonoQ", respectively, such that the final p115 concentration was approximately 20 nM by Western blot. After binding and washing reactions similarly to as in Figure 3, the bead-bound p115 was determined by Western blots and quantitated. (B) Coommassie-stained gels showing the Mono Q p115 preparation used in the binding experiment with a rat his-p115 standard (left panel) and the proteins on each type of beads at the concentration employed (right panel). (C) ER-to-Golgi transport reconstitution in semi-intact NRK cells, where VSV-G transport is indicated by conversion of VSV G cargo from the endoglycosidase H-sensitive to –resistant form. The partially purified rat liver Superdex fraction fully reconstituted the assay in the presence of p115-depleted cytosol (closed circles); the Superdex fraction lost its restorative activity when it was depleted with anti-p115 (open circles). (D) Immunoblot analysis of the Superdex fraction, with or without immunodepletion, relative to the starting cytosol and ammonium sulfate cut, and equal protein loading in each lane. Blotting for other species demonstrates selectivity in the purification; rsly1 shows an overall lack of enrichment over the two-step purification, while a 55 kD degradation/truncation product of p115 visible in cytosol on over-exposed blots was removed during the purification. (E) Coommassie–stained gel documenting proteins on the beads for binding studies in part (F) and (G). Stoichiometry of the membrin and rbet1 bands indicated on the gels on the membrin+rbet1 beads was calculated by quantitation relative to BSA standards. (F) Rat liver Superdex fraction was incubated with the beads shown in (E) at approximately 30 nM p115, then unbound p115 was removed by washing and bound p115 determined by Western blotting and quantitation. The graph shows beads used along the bottom and bound p115 on the y-axis. (G) Membrin beads and soluble rbet1 can form a potentiated ternary SNARE complex. Presence of different beads and soluble proteins are indicated below and syntaxin 5 binding is shown on the y axis. Error bars represent standard error of duplicate determinations. (H) Excess Superdex p115 inhibits *in vitro* ER-Golgi transport.

Chapter VII. Discussion

A. P115's SNARE Binding Preferences *in vitro*

Using a gel filtration assay, we have for the first time provided direct evidence that p115 preferentially interacts with monomeric SNARE motifs. Our results demonstrated that p115 binds mammalian ER-Golgi v-SNARE sec22b and t-SNARE rbet1. The fact that p115 can interact with the ΔTM recombinant rbet1 led us to believe that the SNARE motif is the binding site for p115. Further studies with the N-terminal longin domain of sec22b showed that p115 does not interact with this region, suggesting that the SNARE motif accounts for the interactions between p115 and the recombinant ΔTM sec22b. Structural similarities between p115's coiled-coil domain and the SNARE motif suggest that they could form a coiled-coil structure.

It was unexpected that our solution binding method did not detect p115-membrin or p115-syntaxin 5 interactions, which have been demonstrated before using other methods. One possibility is that the highly oligomeric state of syntaxin 5 and membrin blocked p115's access to the SNARE motif. Due to lower affinity binding, p115's interactions with these SNAREs may be transient, and the resulting complexes would be too unstable to be detected by the gel filtration assay.

Since SNARE motifs are the binding sites for p115, and since these motifs are joined into a four-helix-bundle during fusion, p115 might have to dissociate from its bound partner during the formation of a SNARE complex. In support of this hypothesis, our results showed that p115 interacts with rbet1 alone, but not SNARE complexes containing rbet1. In addition, membrin is able to displace p115 from a

pre-formed rbet1-p115 complex. Furthermore, in vitro studies show that soluble monomeric rbet1 can compete p115 off COPII vesicles, suggesting a free monomeric SNARE motif is a major binding site for p115 on membrane.

We have also demonstrated that excess p115 inhibits COPII vesicle tethering and fusion in vitro and Golgi homeostasis in vivo. These findings are consistent with our binding studies, from which we have concluded that p115 needs to dissociate from SNARE complexes before their formation is complete. Excess p115 could potentially impair fusion efficiency by slowing down this removal process. However, it is worth noting that the inhibitory effect of p115 on vesicle fusion has not been observed in previous studies using in vitro systems. p115 purified from rat liver showed no inhibitory effects on the transport of VSV-G to the medial Golgi at 160% of cytosolic level [99], and recombinant bovine p115 purified from insect cells showed no such effects on VSV-G processing at high concentrations, either [50]. One potential explanation for the apparent discrepancy is that our assay specifically measures the homotypic fusion aspect of the VSV-G transport pathway, and employs vesicles in very dilute suspension; this could make it more sensitive to changes in p115 on-off dynamics than a more intact subcellular reconstitution containing local concentration gradients of cofactors and a cytoskeleton. In our hands the in vitro ER-to-Golgi assay was also inhibited by excess p115, but at concentrations exceeding those that inhibited in the vesicle fusion assay. Both assays contained about 30 nM of rat liver cytosolic p115 under normal conditions. Addition of an additional 20 nM of purified recombinant p115 inhibited the fusion assay (representing ~166% of cytosolic, Figure 18D) whereas inhibition of the ER-to-

Golgi transport assay didn't occur until addition of an additional 60 nM of Superdex p115 (representing ~300% of cytosolic, Figure 20H). Fully purified p115 also inhibited the ER-to-Golgi assay, but to a much lesser degree than in the fusion assay. We believe that the fusion assay helped reveal an inhibitory activity of excess p115 not apparent until higher concentrations in other systems.

We did not see as high a level of stimulation by p115 on SNARE complex formation as was observed in previous studies performed with Golgi detergent extract [116]. Many factors could have contributed to this difference. First, our binding studies were carried out with purified proteins as opposed to Golgi extracts. It is possible that certain p115 accessory factors and/or SNARE destabilizing factors are absent in the purified system, resulting in p115 appearing to lose some SNARE assembly function. Another factor is that the embedding of SNAREs in a membrane is important for p115's catalytic action. We did notice, however, that with the addition of p115, the elution of some monomer rbet1 shifted from fractions 32-34 to fractions 26-32 (Figure 12B), suggesting that the SNARE might have undergone conformational changes in the presence of p115. Furthermore, whereas p115 appears to have no instantaneous effect on the formation of SNARE complexes, its pre-incubation with sec22b increases the complex yield by 2~3 fold (Figure 17B). This increase is more or less in agreement with p115's published effects on purified syntaxin 5-GOS-28 complex formation [116]. Based on the evidence, we suspect that instead of a SNARE catalyst, p115 may act as a SNARE chaperone by modifying the SNARE motifs and/or keeping them in an optimal conformation, at least in soluble SNARE assembly reactions. Whether p115 also assembles SNAREs catalytically

when embedded in membranes remains to be experimentally addressed.

B. Model of P115's Mechanism of Action

Taken together, our results support a model in which p115 binds monomeric SNAREs on the membrane to stabilize their conformation and possibly facilitate fusion by catalyzing SNARE-SNARE interactions, and then is displaced as the SNAREs come together. This potential mechanism of action would explain the observed inhibition of trafficking by excess p115 in vitro and in vivo. For a monomeric SNARE, the binding of p115 and the binding of another SNARE could be mutually exclusive, and excess p115 would slow down p115's removal from the forming SNARE complex. The model also provides insights into the observed highly dynamic state of membrane-bound p115 [100] that could indicate synchronization between p115 recruitment/dissociation and the fusion process.

A possible model for molecular events during p115-mediated docking and fusion of vesicles is that p115 is recruited to the membrane by the dimer's globular head and/or CC1 domains via binding to Rab1 or SNAREs (Figure 21A). P115 could then use a free SNARE-interacting domain (either CC1 or CC4) or the head domain to initiate interactions with SNAREs or Rab1 on the opposing membrane (green arrows), thus tethering the vesicles together. Subsequently, p115 could align the SNAREs on juxtaposed membranes by conformational changes within the p115 molecule. It is also possible that p115 never directly bridges the two membranes, but works solely on the vesicle membrane to enhance the efficiency of SNARE assembly by maintaining their reactivity and concentrating monomeric SNAREs at

fusion sites where Rab1 is active (Figure 21B). This would make p115 less of a traditional 'tether', and more of a chaperone and/or catalyst for SNARE-mediated fusion. Further studies will be essential to define the details of molecular tethering and SNARE coupling by p115.

C. Significance to the Field

Despite the important role of tethers in fusion, a lot remains unknown about their working mechanisms [54, 65]. The recently solved crystal structure of Dsl1 complex provides perhaps the first detailed view of the function of a tether on a molecular basis [70], and parallels have been drawn between Dsl1 and other MTCs in the CATCHR family that have similar interactions with SNAREs [68, 139, 140]. The presence of the homologous SNARE-interacting MUN domain, for example, suggests a shared SNARE-related function [142, 143]. However, it is still unclear how the recruitment of Dsl1 is regulated without an interacting Rab [74], and no coat component that interacts with exocyst has been identified [49]. Despite the extensively characterized interactions between MTCs and other trafficking-related proteins, the functional relevance of these interactions are not all known, and a clear picture of the coordinated collaboration between Rabs, tethers, coats, and SNAREs is yet to emerge.

Comparing to the MTCs, rod-like tethering factors are relatively understudied, and their interactions with other trafficking components, in particular the SNARE proteins, are less defined [49 and Table 1]. It is unclear whether Golgins function as *bona fide* tethers by assembling membrane-bridging complexes, or

facilitate vesicle tethering and fusion through other means (e. g. by acting as SNARE catalysts), and the two possibilities are not mutually exclusive. Rod-like tethers, too, display strong structural homologies such as globular head domains with Rab binding sites, and predominant, elongated coil-coils with multiple flexible 'hinge' regions [53, 54]. Aside from p115, other SNARE interactions have been reported for Golgins. GM130, for example, has been shown to bind Syntaxin 5 and regulate its SNARE activity [84], and tether GCC185 interacts with syntaxin 16 [141]. It is therefore possible that this group of tethers interact with SNAREs in a similar manner as p115 and share a similar mode of action.

We hope our characterization of p115-SNARE interactions leads to a better understanding of p115 mechanism of action, as well as providing new insights into the general functions of Golgin tethers and their role in the secretory pathway. In this study we provide evidence for a potential novel model of action for the tether protein p115, in which p115 binds monomeric SNAREs on the membrane, possibly facilitates fusion by catalyzing SNARE-SNARE interactions, and then is displaced as the SNAREs come together. The fact that p115 binds the SNARE motif through two SNARE homologous domains suggests that these bindings have some of the properties of SNARE-SNARE interactions, and the CC1- or CC4-SNARE complex may structurally resemble a partial SNARE bundle. Through these interactions p115 might stabilize the SNARE motif in a partially structured conformation and prime it for more efficient assembly into a SNARE complex. A more detailed structural analysis of the p115-rbet1 complex might reveal more insights into p115's SNARE-related function.

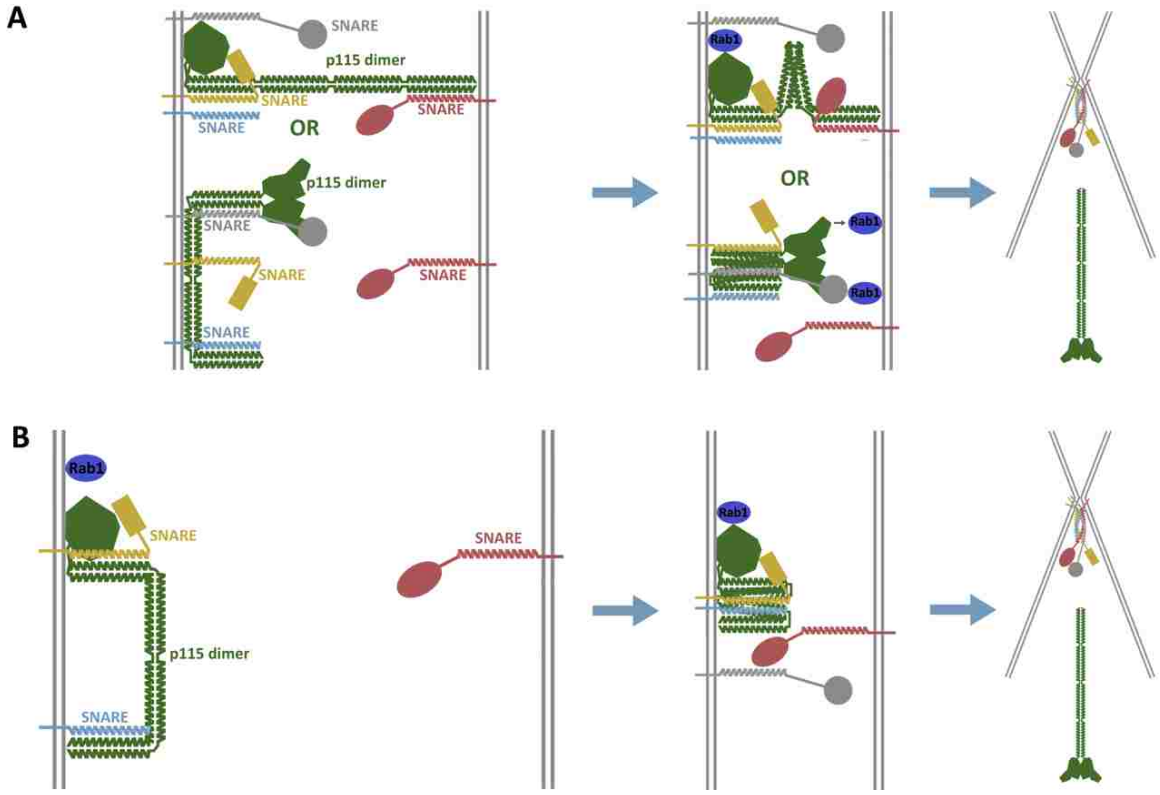

Figure 21. Possible mechanisms of action of p115. (A) Two membrane-bridging models for p115. P115 dimer (green) is recruited to membranes by interacting with monomeric SNAREs (yellow and red, gray and cyan) through the CC1 and/or CC4 domains, and/or by binding to Rab1 (dark blue) through the globular head domain. In the upper version, p115 also binds a monomeric SNARE on an opposing membrane using its free CC4 domain. The binding of p115's globular head domain to Rab1 on the same or opposing membrane causes a conformational change in the tail region of p115, which shortens the distance between membranes and places the N-termini of the SNARE motifs in close proximity. The formation of the four-helix bundle expels p115. (B) P115 dimer captures and concentrates the SNAREs on the same membrane (yellow and cyan) using both the CC1 and CC4 domains. Conformational changes bring the juxtaposed SNAREs together, as well as prime them to interact with SNAREs on the opposing membrane. Our data does not distinguish between the displayed scenarios and several similar variations. The cartoon representation of p115 was adapted from the p115 structure with the acidic C-terminus omitted (106).

References

1. Martinez-Menarguez JA, Geuze HJ, Slot JW, Klumperman J. Vesicular tubular clusters between the ER and Golgi mediate concentration of soluble secretory proteins by exclusion front COPI-coated vesicles. Cell 1999;98(1):81-90.

2. Martoglio B, Dobberstein B. Signal sequences: more than just greasy peptides. Trends in Cell Biology 1998;8(10):410-415.

3. Xu DL, Hay JC. Reconstitution of COPII vesicle fusion to generate a pre-Golgi intermediate compartment. Journal of Cell Biology 2004;167(6):997-1003.

4. Bonifacino JS, Lippincott-Schwartz J. Opinion - Coat proteins: shaping membrane transport. Nature Reviews Molecular Cell Biology 2003;4(5):409-414.

5. Lee C, Goldberg J. Structure of Coatomer Cage Proteins and the Relationship among COPI, COPII, and Clathrin Vesicle Coats. Cell 2010;142(1):123-132.

6. Cosson P, Letourneur F. Coatomer (COPI)-coated vesicles: role in intracellular transport and protein sorting. Current Opinion in Cell Biology 1997;9(4):484-487.

7. Lee MCS, Miller EA. Molecular mechanisms of COPII vesicle formation. Seminars in Cell & Developmental Biology 2007;18(4):424-434.

8. Hughes H, Stephens DJ. Assembly, organization, and function of the COPII coat. Histochemistry and Cell Biology 2008;129(2):129-151.

9. Edeling MA, Smith C, Owen D. Life of a clathrin coat: insights from clathrin and AP structures. Nature Reviews Molecular Cell Biology 2006;7(1):32-44.

10. Pearse BM. Clathrin: a unique protein associated with intracellular transfer of membrane by coated vesicles. Proc Natl Acad Sci U S A 1976;73(4):1255-1259.

11. Brodsky FM, Chen CY, Knuehl C, Towler MC, Wakeham DE. Biological basket weaving: formation and function of clathrin-coated vesicles. Annu Rev Cell Dev Biol 2001;17:517-568.

12. Ungar D, Hughson FM. SNARE protein structure and function. Annu Rev Cell Dev Biol 2003;19:493-517.

13. Sutton RB, Fasshauer D, Jahn R, Brunger AT. Crystal structure of a SNARE complex involved in synaptic exocytosis at 2.4 A resolution. Nature 1998;395(6700):347-353.

14. Sorensen JB, Wiederhold K, Muller EM, Milosevic I, Nagy G, de Groot BL, Grubmuller H, Fasshauer D. Sequential N- to C-terminal SNARE complex assembly drives priming and fusion of secretory vesicles. EMBO J 2006;25(5):955-966.

15. Hanson PI, Heuser JE, Jahn R. Neurotransmitter release - four years of SNARE complexes. Curr Opin Neurobiol 1997;7(3):310-315.

16. Fasshauer D, Margittai M. A transient N-terminal interaction of SNAP-25 and syntaxin nucleates SNARE assembly. J Biol Chem 2004;279(9):7613-7621.

17. Antonin W, Fasshauer D, Becker S, Jahn R, Schneider TR. Crystal structure of the endosomal SNARE complex reveals common structural principles of all SNAREs. Nat Struct Biol 2002;9(2):107-111.

18. Fasshauer D, Sutton RB, Brunger AT, Jahn R. Conserved structural features of the synaptic fusion complex: SNARE proteins reclassified as Q- and R-SNAREs. Proc Natl Acad Sci U S A 1998;95(26):15781-15786.

19. May AP, Whiteheart SW, Weis WI. Unraveling the mechanism of the vesicle transport ATPase NSF, the N-ethylmaleimide-sensitive factor. J Biol Chem 2001;276(25):21991-21994.

20. Sollner T, Bennett MK, Whiteheart SW, Scheller RH, Rothman JE. A protein assembly-disassembly pathway in vitro that may correspond to sequential steps of synaptic vesicle docking, activation, and fusion. Cell 1993;75(3):409-418.

21. Sudhof TC, Rothman JE. Membrane fusion: grappling with SNARE and SM proteins. Science 2009;323(5913):474-477.

22. Misura KM, Scheller RH, Weis WI. Three-dimensional structure of the neuronal-Sec1-syntaxin 1a complex. Nature 2000;404(6776):355-362.

23. Munson M. To protect or reject. Elife;3:e03374.

24. Lobingier BT, Nickerson DP, Lo SY, Merz AJ. SM proteins Sly1 and Vps33 co-assemble with Sec17 and SNARE complexes to oppose SNARE disassembly by Sec18. Elife;3:e02272.

25. Starai VJ, Hickey CM, Wickner W. HOPS proofreads the trans-SNARE complex for yeast vacuole fusion. Mol Biol Cell 2008;19(6):2500-2508.

26. Fernandez I, Ubach J, Dulubova I, Zhang X, Sudhof TC, Rizo J. Three-dimensional structure of an evolutionarily conserved N-terminal domain of syntaxin 1A. Cell 1998;94(6):841-849.

27. Bennett MK, Garcia-Arraras JE, Elferink LA, Peterson K, Fleming AM, Hazuka CD, Scheller RH. The syntaxin family of vesicular transport receptors. Cell 1993;74(5):863-873.

28. Misura KM, Bock JB, Gonzalez LC, Jr., Scheller RH, Weis WI. Three-dimensional structure of the amino-terminal domain of syntaxin 6, a SNAP-25 C homolog. Proc Natl Acad Sci U S A 2002;99(14):9184-9189.

29. Xu D, Joglekar AP, Williams AL, Hay JC. Subunit structure of a mammalian ER/Golgi SNARE complex. J Biol Chem 2000;275(50):39631-39639.

30. Nicholson KL, Munson M, Miller RB, Filip TJ, Fairman R, Hughson FM. Regulation of SNARE complex assembly by an N-terminal domain of the t-SNARE Sso1p. Nat Struct Biol 1998;5(9):793-802.

31. Parlati F, Weber T, McNew JA, Westermann B, Sollner TH, Rothman JE. Rapid and efficient fusion of phospholipid vesicles by the alpha-helical core of a SNARE complex in the absence of an N-terminal regulatory domain. Proc Natl Acad Sci U S A 1999;96(22):12565-12570.

32. Gonzalez LC, Jr., Weis WI, Scheller RH. A novel snare N-terminal domain revealed by the crystal structure of Sec22b. J Biol Chem 2001;276(26):24203-24211.

33. Uemura T, Sato MH, Takeyasu K. The longin domain regulates subcellular targeting of VAMP7 in Arabidopsis thaliana. FEBS Lett 2005;579(13):2842-2846.

34. Hasegawa H, Zinsser S, Rhee Y, Vik-Mo EO, Davanger S, Hay JC. Mammalian Ykt6 is a neuronal SNARE targeted to a specialized compartment by its profilin-like amino terminal domain. Molecular Biology of the Cell 2003;14(2):698-720.

35. Fukasawa M, Varlamov O, Eng WS, Sollner TH, Rothman JE. Localization and activity of the SNARE Ykt6 determined by its regulatory domain and palmitoylation. Proc Natl Acad Sci U S A 2004;101(14):4815-4820.

36. Liu YT, Flanagan JJ, Barlowe C. Sec22p export from the endoplasmic reticulum is independent of SNARE pairing. Journal of Biological Chemistry 2004;279(26):27225-27232.

37. Mancias JD, Goldberg J. The transport signal on Sec22 for packaging into COPII-coated vesicles is a conformational epitope. Mol Cell 2007;26(3):403-414.

38. Ayong L, Raghavan A, Schneider TG, Taraschi TF, Fidock DA, Chakrabarti D. The Longin Domain Regulates the Steady-State Dynamics of Sec22 in Plasmodium falciparum. Eukaryotic Cell 2009;8(9):1330-1340.

39. Wen W, Chen L, Wu H, Sun X, Zhang M, Banfield DK. Identification of the yeast R-SNARE Nyv1p as a novel longin domain-containing protein. Mol Biol Cell 2006;17(10):4282-4299.

40. Weber T, Zemelman BV, McNew JA, Westermann B, Gmachl M, Parlati F, Sollner TH, Rothman JE. SNAREpins: minimal machinery for membrane fusion. Cell 1998;92(6):759-772.

41. Fasshauer D, Antonin W, Subramaniam V, Jahn R. SNARE assembly and disassembly exhibit a pronounced hysteresis. Nat Struct Biol 2002;9(2):144-151.

42. Laufman O, Hong W, Lev S. The COG complex interacts with multiple Golgi SNAREs and enhances fusogenic assembly of SNARE complexes. J Cell Sci;126(Pt 6):1506-1516.

43. McNew JA, Parlati F, Fukuda R, Johnston RJ, Paz K, Paumet F, Sollner TH, Rothman JE. Compartmental specificity of cellular membrane fusion encoded in SNARE proteins. Nature 2000;407(6801):153-159.

44. Parlati F, McNew JA, Fukuda R, Miller R, Sollner TH, Rothman JE. Topological restriction of SNARE-dependent membrane fusion. Nature 2000;407(6801):194-198.

45. Fasshauer D, Antonin W, Margittai M, Pabst S, Jahn R. Mixed and non-cognate SNARE complexes. Characterization of assembly and biophysical properties. J Biol Chem 1999;274(22):15440-15446.

46. Trahey M, Hay JC. Transport vesicle uncoating: it's later than you think. F1000 Biol Rep;2:47.

47. Cai H, Yu S, Menon S, Cai Y, Lazarova D, Fu C, Reinisch K, Hay JC, Ferro-Novick S. TRAPPI tethers COPII vesicles by binding the coat subunit Sec23. Nature 2007;445(7130):941-944.

48. Whyte JR, Munro S. Vesicle tethering complexes in membrane traffic. J Cell Sci 2002;115(Pt 13):2627-2637.

49. Sztul E, Lupashin V. Role of vesicle tethering factors in the ER-Golgi membrane traffic. FEBS Lett 2009;583(23):3770-3783.

50. Allan BB, Moyer BD, Balch WE. Rab1 recruitment of p115 into a cis-SNARE complex: programming budding COPII vesicles for fusion. Science 2000;289(5478):444-448.

51. Guo W, Roth D, Walch-Solimena C, Novick P. The exocyst is an effector for Sec4p, targeting secretory vesicles to sites of exocytosis. Embo Journal 1999;18(4):1071-1080.

52. Bentley M, Liang Y, Mullen K, Xu D, Sztul E, Hay JC. SNARE status regulates tether recruitment and function in homotypic COPII vesicle fusion. J Biol Chem 2006;281(50):38825-38833.

53. Chan EKL, Fritzler MJ. Golgins: coiled-coil-rich proteins associated with the Golgi Complex. Electronic Journal of Biotechnology 1998; 1(2):1-10.

54. Lupashin V, Sztul E. Golgi tethering factors. Biochimica Et Biophysica Acta-Molecular Cell Research 2005;1744(3):325-339.

55. Orci L, Perrelet A, Rothman JE. Vesicles on strings: Morphological evidence for processive transport within the Golgi stack. Proceedings of the National Academy of Sciences of the United States of America 1998;95(5):2279-2283.

56. Waters MG, Clary DO, Rothman JE. A Novel 115-Kd Peripheral Membrane-Protein Is Required for Intercisternal Transport in the Golgi Stack. Journal of Cell Biology 1992;118(5):1015-1026.

57. Shorter J, Warren G. A role for the vesicle tethering protein, p115, in the post-mitotic stacking of reassembling Golgi cisternae in a cell-free system. Journal of Cell Biology 1999;146(1):57-70.

58. Nakamura N, Rabouille C, Watson R, Nilsson T, Hui N, Slusarewicz P, Kreis TE, Warren G. Characterization of a cis-Golgi matrix protein, GM130. Journal of Cell Biology 1995;131(6):1715-1726.

59. Barr FA, Nakamura N, Warren G. Mapping the interaction between GRASP65 and GM130, components of a protein complex involved in the stacking of Golgi cisternae. Embo Journal 1998;17(12):3258-3268.

60. Sonnichsen B, Lowe M, Levine T, Jamsa E, Dirac-Svejstrup B, Warren G. A role for giantin in docking COPI vesicles to Golgi membranes. J Cell Biol 1998;140(5):1013-1021.

61. Alvarez C, Garcia-Mata R, Hauri HP, Sztul E. The p115-interactive proteins GM130 and giantin participate in endoplasmic reticulum-Golgi traffic. J Biol Chem 2001;276(4):2693-2700.

62. Hong WJ, Lev S. Tethering the assembly of SNARE complexes. Trends in Cell Biology 2014;24(1):35-43.

63. Waters MG, Pfeffer SR. Membrane tethering in intracellular transport. Curr Opin Cell Biol 1999;11(4):453-459.

64. Yu IM, Hughson FM. Tethering Factors as Organizers of Intracellular Vesicular Traffic. Annual Review of Cell and Developmental Biology, Vol 26 2010;26:137-156.

65. Brocker C, Engelbrecht-Vandre S, Ungermann C. Multisubunit Tethering Complexes and Their Role in Membrane Fusion. Current Biology 2010;20(21):R943-R952.

66. Smith RD, Lupashin VV. Role of the conserved oligomeric Golgi (COG) complex in protein glycosylation. Carbohydrate Research 2008;343(12):2024-2031.

67. Liu JL, Guo W. The exocyst complex in exocytosis and cell migration. Protoplasma 2012;249(3):587-597.

68. Heider MR, Munson M. Exorcising the exocyst complex. Traffic;13(7):898-907.

69. Spang A. The DSL1 Complex: The Smallest but Not the Least CATCHR. Traffic 2012;13(7):908-913.

70. Ren Y, Yip CK, Tripathi A, Huie D, Jeffrey PD, Walz T, Hughson FM. A Structure-Based Mechanism for Vesicle Capture by the Multisubunit Tethering Complex Dsl1. Cell 2009;139(6):1119-1129.

71. Stenmark H. Rab GTPases as coordinators of vesicle traffic. Nature Reviews Molecular Cell Biology 2009;10(8):513-525.

72. Barr FA. Rab GTPases and membrane identity: Causal or inconsequential? Journal of Cell Biology 2013;202(2):191-199.

73. Pfeffer SR. Rab GTPase regulation of membrane identity. Curr Opin Cell Biol;25(4):414-419.

74. Cai H, Reinisch K, Ferro-Novick S. Coats, tethers, Rabs, and SNAREs work together to mediate the intracellular destination of a transport vesicle. Dev Cell 2007;12(5):671-682.

75. Rosing M, Ossendorf E, Rak A, Barnekow A. Giantin interacts with both the small GTPase Rab6 and Rab1. Experimental Cell Research 2007;313(11):2318-2325.

76. Miller VJ, Sharma P, Kudlyk TA, Frost L, Rofe AP, Watson IJ, Duden R, Lowe M, Lupashin VV, Ungar D. Molecular Insights into Vesicle Tethering at the Golgi by the

Conserved Oligomeric Golgi (COG) Complex and the Golgin TATA Element Modulatory Factor (TMF). Journal of Biological Chemistry 2013;288(6):4229-4240.

77. Siniossoglou S, Pelham HRB. An effector of Ypt6p binds the SNARE Tlg1p and mediates selective fusion of vesicles with late Golgi membranes. Embo Journal 2001;20(21):5991-5998.

78. Conibear E, Cleck JN, Stevens TH. Vps51p mediates the association of the GARP (Vps52/53/54) complex with the late Golgi t-SNARE Tlg1p. Molecular Biology of the Cell 2003;14(4):1610-1623.

79. Wurmser AE, Sato TK, Emr SD. New component of the vacuolar class C-Vps complex couples nucleotide exchange on the Ypt7 GTPase to SNARE-dependent docking and fusion. Journal of Cell Biology 2000;151(3):551-562.

80. Seals DF, Eitzen G, Margolis N, Wickner WT, Price A. A Ypt/Rab effector complex containing the Sec1 homolog Vps33p is required for homotypic vacuole fusion. Proceedings of the National Academy of Sciences of the United States of America 2000;97(17):9402-9407.

81. Peplowska K, Markgraf DF, Ostrowicz CW, Bange G, Ungermann C. The CORVET tethering complex interacts with the yeast Rab5 homolog Vps21 and is involved in endo-lysosomal biogenesis. Developmental Cell 2007;12(5):739-750.

82. Brunet S, Sacher M. Are all multisubunit tethering complexes bona fide tethers? Traffic;15(11):1282-1287.

83. Sacher M, Jiang Y, Barrowman J, Scarpa A, Burston J, Zhang L, Schieltz D, Yates JR, Abeliovich H, Ferro-Novick S. TRAPP, a highly conserved novel complex on the cis-Golgi that mediates vesicle docking and fusion. Embo Journal 1998;17(9):2494-2503.

84. Diao A, Frost L, Morohashi Y, Lowe M. Coordination of golgin tethering and SNARE assembly - GM130 binds syntaxin 5 in a p115-regulated manner. Journal of Biological Chemistry 2008;283(11):6957-6967.

85. Sivaram MVS, Saporita JA, Furgason MLM, Boettcher AJ, Munson M. Dimerization of the exocyst protein Sec6p and its interaction with the t-SNARE Sec9p. Biochemistry 2005;44(16):6302-6311.

86. Morgera F, Sallah MR, Dubuke ML, Gandhi P, Brewer DN, Carr CM, Munson M. Regulation of exocytosis by the exocyst subunit Sec6 and the SM protein Sec1. Molecular Biology of the Cell 2012;23(2):337-346.

87. Shestakova A, Suvorova E, Pavliv O, Khaidakova G, Lupashin V. Interaction of the conserved oligomeric Golgi complex with t-SNARE Syntaxin5a/Sed5 enhances

intra-Golgi SNARE complex stability. Journal of Cell Biology 2007;179(6):1179-1192.

88. Simonsen A, Gaullier JM, D'Arrigo A, Stenmark H. The Rab5 effector EEA1 interacts directly with syntaxin-6. Journal of Biological Chemistry 1999;274(41):28857-28860.

89. McBride HM, Rybin V, Murphy C, Giner A, Teasdale R, Zerial M. Oligomeric complexes link Rab5 effectors with NSF and drive membrane fusion via interactions between EEA1 and syntaxin 13. Cell 1999;98(3):377-386.

90. Mills IG, Urbe S, Clague MJ. Relationships between EEA1 binding partners and their role in endosome fusion. Journal of Cell Science 2001;114(10):1959-1965.

91. Laufman O, Hong WJ, Lev S. The COG complex interacts directly with Syntaxin 6 and positively regulates endosome-to-TGN retrograde transport. Journal of Cell Biology 2011;194(3):459-472.

92. Oka T, Ungar D, Hughson FM, Krieger M. The COG and COPI complexes interact to control the abundance of GEARs, a subset of Golgi integral membrane proteins. Molecular Biology of the Cell 2004;15(5):2423-2435.

93. Laufman O, Hong WJ, Lev S. The COG complex interacts with multiple Golgi SNAREs and enhances fusogenic assembly of SNARE complexes. Journal of Cell Science 2013;126(6):1506-1516.

94. Nakajima H, Hirata A, Ogawa Y, Yonehara T, Yoda K, Yamasaki M. A Cytoskeleton-Related Gene, Uso1, Is Required for Intracellular Protein-Transport in Saccharomyces-Cerevisiae. Journal of Cell Biology 1991;113(2):245-260.

95. Barroso M, Nelson DS, Sztul E. Transcytosis-Associated Protein (Tap)/P115 Is a General Fusion Factor Required for Binding of Vesicles to Acceptor Membranes. Proceedings of the National Academy of Sciences of the United States of America 1995;92(2):527-531.

96. Sapperstein SK, Lupashin VV, Schmitt HD, Waters MG. Assembly of the ER to Golgi SNARE complex requires Uso1p. Journal of Cell Biology 1996;132(5):755-767.

97. Barlowe C. Coupled ER to Golgi transport reconstituted with purified cytosolic proteins. Journal of Cell Biology 1997;139(5):1097-1108.

98. Cao XC, Ballew N, Barlowe C. Initial docking of ER-derived vesicles requires Uso1p and Ypt1p but is independent of SNARE proteins. Embo Journal 1998;17(8):2156-2165.

99. Alvarez C, Fujita H, Hubbard A, Sztul E. ER to Golgi transport: Requirement for p115 at a pre-Golgi VTC stage. Journal of Cell Biology 1999;147(6):1205-1221.

100. Brandon E, Szul T, Alvarez C, Grabski R, Benjamin R, Kawai R, Sztul E. On and off membrane dynamics of the endoplasmic reticulum-golgi tethering factor p115 in vivo. Mol Biol Cell 2006;17(7):2996-3008.

101. Sapperstein SK, Walter DM, Grosvenor AR, Heuser JE, Waters MG. P115 Is a General Vesicular Transport Factor-Related to the Yeast Endoplasmic-Reticulum to Golgi Transport Factor Uso1p. Proceedings of the National Academy of Sciences of the United States of America 1995;92(2):522-526.

102. Yamakawa H, Seog DH, Yoda K, Yamasaki M, Wakabayashi T. Uso1 protein is a dimer with two globular heads and a long coiled-coil tail. Journal of Structural Biology 1996;116(3):356-365.

103. Garcia-Mata R, Gao Y, Alvarez C, Sztul ES. The membrane transport factor p115 recycles only between homologous compartments in intact heterokaryons. Eur J Cell Biol 2000;79(4):229-239.

104. An Y, Chen CY, Moyer B, Rotkiewicz P, Elsliger MA, Godzik A, Wilson IA, Balch WE. Structural and Functional Analysis of the Globular Head Domain of p115 Provides Insight into Membrane Tethering. Journal of Molecular Biology 2009;391(1):26-41.

105. Striegl H, Roske Y, Kummel D, Heinemann U. Unusual Armadillo Fold in the Human General Vesicular Transport Factor p115. Plos One 2009;4(2).

106. Beard M, Satoh A, Shorter J, Warren G. A cryptic Rab1-binding site in the p115 tethering protein (vol 280, pg 25840, 2005). Journal of Biological Chemistry 2006;281(38):28488-28488.

107. Nelson DS, Alvarez C, Gao YS, Garcia-Mata R, Fialkowski E, Sztul E. The membrane transport factor TAP/p115 cycles between the Golgi and earlier secretory compartments and contains distinct domains required for its localization and function. Journal of Cell Biology 1998;143(2):319-331.

108. Nakamura N, Lowe M, Levine TP, Rabouille C, Warren G. The vesicle docking protein p115 binds GM130, a cis-Golgi matrix protein, in a mitotically regulated manner. Cell 1997;89(3):445-455.

109. Shorter JG, Dirac-Svejstrup B, Waters G, Warren G. Phosphorylation of the vesicle tethering protein p115 by a casein kinase II-like enzyme is required for Golgi reassembly from isolated mitotic fragments. Molecular Biology of the Cell 2000;11:282A-282A.

110. Linstedt AD, Jesch SA, Mehta A, Lee TH, Garcia-Mata R, Nelson DS, Sztul E. Binding relationships of membrane tethering components - The giantin N terminus and the GM130 N terminus compete for binding to the p115 C terminus. Journal of Biological Chemistry 2000;275(14):10196-10201.

111. Lesa GM, Seemann J, Shorter J, Vandekerckhove J, Warren G. The amino-terminal domain of the Golgi protein Giantin interacts directly with the vesicle-tethering protein p115. Journal of Biological Chemistry 2000;275(4):2831-2836.

112. Satoh A, Warren G. In situ cleavage of the acidic domain from the p115 tether inhibits exocytic transport. Traffic 2008;9(9):1522-1529.

113. Puthenveedu MA, Linstedt AD. Gene replacement reveals that p115/SNARE interactions are essential for Golgi biogenesis. Proceedings of the National Academy of Sciences of the United States of America 2004;101(5):1253-1256.

114. Grabski R, Balklava Z, Wyrozumska P, Szul T, Brandon E, Alvarez C, Holloway ZG, Sztul E. Identification of a functional domain within the p115 tethering factor that is required for Golgi ribbon assembly and membrane trafficking. Journal of Cell Science 2012;125(8):1896-1909.

115. Sinka R, Gillingham AK, Kondylis V, Munro S. Golgi coiled-coil proteins contain multiple binding sites for Rab family G proteins. Journal of Cell Biology 2008;183(4):607-615.

116. Shorter J, Beard MB, Seemann J, Dirac-Svejstrup AB, Warren G. Sequential tethering of Golgins and catalysis of SNAREpin assembly by the vesicle-tethering protein p115. Journal of Cell Biology 2002;157(1):45-62.

117. Garcia-Mata R, Sztul E. The membrane-tethering protein p115 interacts with GBF1, an ARF guanine-nucleotide-exchange factor. Embo Reports 2003;4(3):320-325.

118. Monetta P, Slavin F, Romero N, Alvarez C. Rab1b interacts with GBF1 and modulates both ARR dynamics and COPI association. Molecular Biology of the Cell 2007;18(7):2400-2410.

119. Sohda M, Misumi Y, Yoshimura S, Nakamura N, Fusano T, Ogata S, Sakisaka S, Ikehara Y. The interaction of two tethering factors, p115 and COG complex, is required for Golgi integrity. Traffic 2007;8(3):270-284.

120. Guo Y, Linstedt AD. Binding of the vesicle docking protein p115 to the GTPase Rab1b regulates membrane recruitment of the COPI vesicle coat. Cell Logist;3:e27687.

121. Kim S, Hill A, Warman ML, Smits P. Golgi disruption and early embryonic lethality in mice lacking USO1. Plos One;7(11):e50530.

122. Sohda M, Misumi Y, Yoshimura S, Nakamura N, Fusano T, Sakisaka S, Ogata S, Fujimoto J, Kiyokawa N, Ikehara Y. Depletion of vesicle-tethering factor p115 causes mini-stacked Golgi fragments with delayed protein transport. Biochem Biophys Res Commun 2005;338(2):1268-1274.

123. Morsomme P, Riezman H. The Rab GTPase Ypt1p and tethering factors couple protein sorting at the ER to vesicle targeting to the Golgi apparatus. Dev Cell 2002;2(3):307-317.

124. Hu C, Ahmed M, Melia TJ, Sollner TH, Mayer T, Rothman JE. Fusion of cells by flipped SNAREs. Science 2003;300(5626):1745-1749.

125. Grabski R, Hay J, Sztul E. Tethering factor P115: a new model for tether-SNARE interactions. Bioarchitecture;2(5):175-180.

126. Zagouras P, Rose JK. Dynamic Equilibrium between Vesicular Stomatitis-Virus Glycoprotein Monomers and Trimers in the Golgi and at the Cell-Surface. Journal of Virology 1993;67(12):7533-7538.

127. Schwaninger R, Beckers CJM, Balch WE. Sequential Transport of Protein between the Endoplasmic-Reticulum and Successive Golgi Compartments in Semi-Intact Cells. Journal of Biological Chemistry 1991;266(20):13055-13063.

128. Stroupe C, Collins KM, Fratti RA, Wickner W. Purification of active HOPS complex reveals its affinities for phosphoinositides and the SNARE Vam7p. Embo Journal 2006;25(8):1579-1589.

129. Laage R, Ungermann C. The N-terminal domain of the t-SNARE Vam3p coordinates priming and docking in yeast vacuole fusion. Molecular Biology of the Cell 2001;12(11):3375-3385.

130. Weimbs T, Low SH, Chapin SJ, Mostov KE, Bucher P, Hofmann K. A conserved domain is present in different families of vesicular fusion proteins: A new superfamily. Proceedings of the National Academy of Sciences of the United States of America 1997;94(7):3046-3051.

131. Tochio H, Tsui MMK, Banfield DK, Zhang MJ. An autoinhibitory mechanism for nonsyntaxin SNARE proteins revealed by the structure of Ykt6p. Science 2001;293(5530):698-702.

132. Martinez-Arca S, Alberts P, Zahraoui A, Louvard D, Galli T. Role of tetanus neurotoxin insensitive vesicle-associated membrane protein (TI-VAMP) in vesicular

transport mediating neurite outgrowth. Journal of Cell Biology 2000;149(4):889-899.

133. Martinez-Arca S, Rudge R, Vacca M, Raposo G, Camonis J, Proux-Gillardeaux V, Daviet L, Formstecher E, Hamburger A, Filippini F, D'Esposito M, Galli T. A dual mechanism controlling the localization and function of exocytic v-SNAREs. Proceedings of the National Academy of Sciences of the United States of America 2003;100(15):9011-9016.

134. Antonin W, Dulubova I, Arac D, Pabst S, Plitzner J, Rizo J, Jahn R. The N-terminal domains of syntaxin 7 and vti1b form three-helix bundles that differ in their ability to regulate SNARE complex assembly. Journal of Biological Chemistry 2002;277(39):36449-36456.

135. Mossessova E, Bickford LC, Goldberg J. SNARE selectivity of the COPII coat. Cell 2003;114(4):483-495.

136. Bentley M, Nycz DC, Joglekar A, Fertschai I, Malli R, Graier WF, Hay JC. Vesicular Calcium Regulates Coat Retention, Fusogenicity, and Size of Pre-Golgi Intermediates. Molecular Biology of the Cell 2010;21(6):1033-1046.

137. Seemann J, Jokitalo EJ, Warren G. The role of the tethering proteins p115 and GM130 in transport through the Golgi apparatus in vivo. Molecular Biology of the Cell 2000;11(2):635-645.

138. Moyer BD, Allan BB, Balch WE. Rab1 interaction with a GM130 effector complex regulates COPII vesicle cis-Golgi tethering. Traffic 2001;2(4):268-276.

139. Lees JA, Yip CK, Walz T, Hughson FM. Molecular organization of the COG vesicle tethering complex. Nature Structural & Molecular Biology 2010;17(11):1292-U1139.

140. Arasaki K, Takagi D, Furuno A, Sohda M, Misumi Y, Wakana Y, Inoue H, Tagaya M. A new role for RINT-1 in SNARE complex assembly at the trans-Golgi network in coordination with the COG complex. Molecular Biology of the Cell 2013;24(18):2907-2917.

141. Ganley IG, Espinosa E, Pfeffer SR. A syntaxin 10-SNARE complex distinguishes two distinct transport routes from endosomes to the trans-Golgi in human cells. Journal of Cell Biology 2008;180(1):159-172.

142. Pei JM, Ma C, Rizo J, Grishin NV. Remote Homology between Munc13 MUN Domain and Vesicle Tethering Complexes. Journal of Molecular Biology 2009;391(3):509-517.

143. Weninger K, Bowen ME, Chu S, Brunger AT. Single-molecule studies of SNARE complex assembly reveal parallel and antiparallel configurations. Proc Natl Acad Sci U S A 2003;100(25):14800-14805.